Medical University of Varna

Faculty of Pharmacy

Ivaylo Konstantinov Pehlivanov

Self-emulsifying drug delivery systems as a method to enhance the intestinal permeability of alendronate sodium

THESIS SUMMARY

of a PhD thesis for awarding the educational and scientific degree "PHILOSOPHY DOCTOR"
Higher Education Area: 7. Healthcare and Sports
Professional Field: 7.3. Pharmacy
Doctoral Programme: Pharmacology (including Pharmacokinetics and Chemotherapy)

Research Supervisors:
Prof. Kaloyan Georgiev, PhD, DSc
Assoc. Prof. Velichka Andonova, PhD

Varna, 2025

The thesis was discussed at an extended meeting of the Department of Pharmacology, Toxicology, and Pharmacotherapy, Faculty of Pharmacy, Medical University of Varna, held on June 06, 2025, and is intended for public defense on September 11, 2025, at 11:30 AM online via the Webex platform.

Members of the Scientific Jury:

Internal members:

1. Assoc. Prof. Maya Petrova Radeva-Ilieva, PhD, Department of Pharmacology, Toxicology, and Pharmacotherapy, Faculty of Pharmacy, Medical University of Varna, Chair of the Scientific Jury;
2. Assoc. Prof. Viliana Eduardova Guggleva, PhD, Department of Pharmaceutical Technologies, Faculty of Medicine, Medical University of Varna.

External members:

3. Prof. Milen Ventsislavov Dimitrov, PhD, Department of Pharmaceutical Technology and Biopharmacy, Faculty of Pharmacy, Medical University of Sofia;
4. Prof. Krum Stefanov Kafedjiiski, PhD, Department of Pharmaceutical Sciences, Medical College, Trakia University, Stara Zagora;
5. Assoc. Prof. Hristo Tsachev Tsachev, Ph.D, Department of Pharmaceutical and Applied Organic Chemistry, Faculty of Chemistry and Pharmacy, Sofia University "St. Kliment Ohridski" , Sofia

Reserve members:

1. Prof. Bistra Kostova, Ph.D, Department of Pharmaceutical Technology and Biopharmacy, Faculty of Pharmacy, Medical University of Sofia;
2. Assoc. Prof. Nadezhda Rumenova Kirkkeselyan, Ph.D., Department of Pharmacology, Toxicology, and Pharmacotherapy, Faculty of Pharmacy, Medical University of Varna.

The thesis contains 140 pages and is illustrated with 33 tables and 33 figures. The bibliography comprises 301 sources, including 1 in Cyrillic and 300 in Latin script.

The materials for the defense are published on the website of the Medical University of Varna.

Contents

Abreviations

BCS	-	Biopharmaceutical Classification System
O/W	-	Oil/Water
O/W/O	-	Oil/Water/Oil
SDEDDS	-	Self Double Emulsifying Drug Delivery System
SDEDDS -NaALD	-	Self Double Emulsifying Drug Delivery System Loaded with Sodium Alendronate
REC	-	Research Ethics Committee
CMC	-	Critical Micelle Concentration
LBDDS	-	Lipid-Based Drug Delivery Systems
API	-	Active Pharmaceutical Ingredient/s
DF	-	Dosage Form/s
W/O	-	Water/Oil
W/O/W	-	Water/Oil/Water
SAA	-	Surfactant/s
HLB	-	Hydrophilic-Lipophilic Balance
ΔT	-	Temperature Change
C	-	Concentration
C_{oil}	-	Concentration in Oil
C_w	-	Concentration in Water
D	-	Diffusion Coefficient
DLS	-	Dynamic Light Scattering
dQ/dt	-	Diffusion Rate of a Given Quantity of API per Unit Time
Ph. Eur.	-	European Pharmacopoeia
FaSSGF	-	Fasted-State Simulated Gastric Fluid
FaSSIF	-	Fasted-State Simulated Intestinal Fluid
H	-	Membrane Thickness
ICH	-	International Council for Harmonisation of Technical Requirements for Pharmaceuticals for Human Use
K_{distr}	-	Water/Oil Distribution Coefficient
K_e	-	Ebullioscopic Constant
$K_{m/w}$	-	Distribution Coefficient Between Biological Fluid and Biological Membrane at the Absorption Site
LOD	-	Limit of Detection
log P	-	Oil/Water Partition Coefficient
LOQ	-	Limit of Quantification
NaALD	-	Sodium Alendronate
PDI	-	Polydispersity Index
PE	-	Primary O/W Emulsion
ΔG	-	Gibbs Free Energy
ΔH	-	Enthalpy
ΔS	-	Entropy
K	-	Equilibrium Constant

I. INTRODUCTION

Improving bioavailability in oral dosage forms (ODFs) remains a challenge for a significant portion of newly developed active pharmaceutical ingredients (APIs). The majority of these compounds belong to Class II, III, or IV of the Biopharmaceutical Classification System (BCS). Their oral administration is often associated with low bioavailability, high intra- and inter-variability in plasma levels, and a lack of dose proportionality. Several strategies exist to improve drugs oral bioavailability, and one of the most widely used involves incorporation these molecules in lipid-based drug delivery systems (LBDDSs). These systems can enhance dissolution profiles and membrane permeability, often leading to a net increase in bioavailability. Lipid-based systems are among the most effective approaches for improving oral bioavailability of many molecules and may include oil solutions or suspensions, emulsions, lipid nanoparticles, and self-emulsifying systems.

When the dispersed phase is lipid-based, emulsions or dispersions of the oil-in-water (O/W) type are formed in the gastrointestinal tract. Incorporating BCS class II APIs in the inner lipid phase may enhance their solubility. In systems with more complex structures (e.g., W/O/W emulsions or liposomes), BCS class III APIs may improve their mucosal permeability when included in the internal aqueous phase.

Given these advantages, lipid-based systems demonstrate high potential for drug delivery. Although lipid-based drug delivery systems (LBDDS) are not a new concept, their use has expanded in recent years due to the growing number of APIs with formulation challenges.. Nearly 40% of new drug candidates are lipophilic[1], with high molecular weights and poor aqueous solubility. For highly hydrophilic drugs, low membrane permeability is often the limiting factor in gastrointestinal absorption[2]. Additional factors significantly affecting bioavailability include low dissolution rates, first-pass metabolism, pre-absorptive metabolism, and cellular efflux. Despite their high pharmacological activity, many APIs are abandoned in later development stages due to poor bioavailability. A major challenge in pharmaceutical science and practice is formulating these compounds into oral dosage forms that ensure sufficient bioavailability.

[1] Pattewar, S., Deshmukh, P., Patil, A. and Muley, P. (2016) 'IJPSR', International Journal of Pharmaceutical Sciences and Research, 7(2). https://doi.org/10.13040/ijpsr.0975-8232.7(2).443-52

[2] Kolhe, S.M., Patel, L.D., Patel, P.A. and Rajput, A.P. (2016) 'Development and evaluation of solid self double emulsifying drug delivery system (SSDEDDS): A novel approach to enhance bioavailability of BCS class III drugs', Journal of Pharmacy Research, 10(6), pp. 403–409

II. AIM AND OBJECTIVES

1. Aim

The aim of this dissertation is to develop a W/O/W self double-emulsifying drug delivery system (SDEDDS) that enhances the oral bioavailability of alendronate sodium (NaALD).

2. Objectives

To achieve this aim, the following tasks are proposed:

1. To develop and validate a UV-Vis spectrophotometric method for quantitative determination of NaALD in model systems, including evaluating the influence of polysorbate 80 and phosphate buffers on method sensitivity.
2. To optimize the composition of the SDEDDS loaded with alendronate sodium (SDEDDS –NaALD).
   - **2.1.** To determine the water/oil partition coefficient (K_{distr}) and the solubility of NaALD in lipids and surfactants.
   - **2.2.** To determine the hydrophilic-lipophilic balance (HLB) of the primary W/O emulsion.
   - **2.3.** To construct pseudoternary phase diagrams for determining the optimal amount of hydrophilic surfactant in the composition of SDEDDS**.**
   - **2.4.** To evaluate the impact of polymers on the stability of the primary emulsion.
   - **2.5.** To assess the physical and thermodynamic stability of SDEDDS –NaALD.
   - **2.6.** To determine the compatibility of NaALD with the selected excipients in the SDEDDS formulation.
   - **2.7.** To measure the self-emulsification time and dispersibility of SDEDDS – NaALD.
   - **2.8.** To study the rheological behavior of SDEDDS –NaALD.
3. To conduct technological and biopharmaceutical characterization studies on SDEDDS –NaALD formulated in hard gelatin capsules.
   - **3.1.** To evaluate the pharmacopoeial parameters 'Uniformity of mass of single-dose preparations' (Ph. Eur. 11 – 2.9.5) and 'Uniformity of dosage units' (Ph. Eur. 11 – 2.9.40) for hard gelatin capsules containing SDEDDS –NaALD.
   - **3.2.** To evaluate the self-emulsification time and dispersibility of hard gelatin capsules with SDEDDS –NaALD in biomimetic media.
   - **3.3.** To study the in vitro permeation of NaALD from hard gelatin capsules containing SDEDDS –NaALD through dialisys and biomimetic membrane.
4. To determine the amount of NaALD excreted in the urine of laboratory animals following oral administration of optimized SDEDDS–NaALD formulations by developing and validating an HPLC-UV/Vis method for detection of the drug in biological matrices.

III. MATERIALS AND METHODS

1. Materials

The following materials were used:

- ✓ Alendronate sodium, monosodium salt trihydrate (>99.7%, USP-NF, BP, Ph. Eur., Polpharma S.A., Poland, NaALD);
- ✓ Gum arabic (acaciae gummi, Ph. Eur., Himax Pharma Ltd., Bulgaria, AG);
- ✓ Acetonitrile (HPLC gradient grade, USP-NF, BP, Ph. Eur., Carlo Erba Reagents srl, Italy, ACN);
- ✓ Granulated soy L-α-lecithin (>97% phosphatidylcholine, ARCOS–Thermo Scientific, Portugal, PCH);
- ✓ Disodium hydrogen phosphate (sodium hydrogen phosphate dodecahydrate cryst., USP-NF, BP, Ph. Eur., Merck, Germany);
- ✓ Dichloromethane stabilized with ethanol (HPLC-isocratic gradient grade, USP-NF, BP, Ph. Eur., Carlo Erba Reagents srl, Italy);
- ✓ Ethanol, absolute (HPLC gradient grade, USP-NF, BP, Ph. Eur., Carlo Erba Reagents srl, Italy);
- ✓ Gelatin (80–100 bloom, USP-NF, BP, Ph. Eur., Panreac Applichem, Spain, G);
- ✓ Iron(III) chloride hexahydrate ($FeCl_3 \cdot 6H_2O$, analytical grade >97%, Chemipur, Poland);
- ✓ Potassium dihydrogen phosphate (USP-NF, BP, Ph. Eur., ChemLab, Belgium);
- ✓ Magnesium chloride hexahydrate ($MgCl_2 \cdot 6H_2O$, USP-NF, BP, Ph. Eur., PPHU, Poland);
- ✓ Cod liver oil (Ph. Eur., FU XII R.Italiana – Marco Viti S.p.A., Italy, CLO);
- ✓ Methanol, absolute (HPLC gradient grade, USP-NF, BP, Ph. Eur., Carlo Erba Reagents srl, Italy);
- ✓ Sodium dihydrogen phosphate (USP-NF, BP, Ph. Eur., ChemLab, Belgium);
- ✓ Sodium hydroxide pellets (NaOH, ≥98%, laboratory grade, Fisher Chemical, Germany);
- ✓ Sodium chloride (NaCl, USP-NF, BP, Ph. Eur., Panreac, Spain);
- ✓ Oleic acid (≥70%, technical grade, Fisher Scientific, UK, OA);
- ✓ Acetic acid, glacial (≥99%, Fisher Scientific, UK);
- ✓ Perchloric acid ($HClO_4$ 70–72%, Chemipur, Poland);
- ✓ Polysorbate 80 (polyoxyethylene sorbitan monooleate, Tween 80, Sigma-Aldrich Chemie GmbH, Germany, PS);
- ✓ Polysorbate 20 (polyoxyethylene sorbitan monolaurate, Tween 20, Sigma-Aldrich Chemie GmbH, Germany, PL);
- ✓ Sorbitan monolaurate (Span 20, Sigma-Aldrich Chemie GmbH, Germany, SL);
- ✓ Sorbitan monooleate (Span 80, Sigma-Aldrich Chemie GmbH, Germany, SM);
- ✓ Medium-chain triglycerides (Caprylic acid C8:0 and Capric acid C10:0 – USP-NF, Now Sports, USA, MCT oil);
- ✓ Whey protein concentrate (WPC 80 – food grade, 81% whey protein, ≤12% lactose monohydrate, Alimco, Poland);
- ✓ Virgin coconut oil (certified # BG-Bio-18, origin: Philippines, BioBalev Ltd., Bulgaria, CO);

- ✓ 9-Fluorenylmethoxycarbonyl chloride (≥98%, Tokyo Chemical Industry Co., Ltd., Japan);
- ✓ Trifluoroacetic acid, pure 99%, HPLC grade, Tokyo Chemical Industry Co., Ltd., Japan;
- ✓ Pamidronate disodium salt, Calbiochem, Merck, Germany;
- ✓ SPE cartridge Bond Elut DEA, 100 mg, 3 mL, Agilent Technologies, USA;
- ✓ Clinical vacutainers with 3.2% citrate buffer, 1.8 mL, Vacusera Disera, Turkey;
- ✓ Cellulose acetate dialysis membrane MWCO 10,000–14,000 Da, 35 mm, Carl Roth GmbH, Germany;
- ✓ Biomimetic membrane PermeaPad® Barrier 25 mm (Germany), purchased from Biomedica Bulgaria Ltd.

2. Equipment

- ✓ Precision electronic balance Kern ABJ 120-4M (0.001 g – 120 g), KERN & Sohn GmbH, Germany;
- ✓ Homogenizer IKA T25 Ultra Turrax with dispersing element Dispersing Element for T 10 basic ULTRA-TURRAX®, Type: S 10 N-8G, IKA – Werke GmbH & Co. KG, Germany;
- ✓ Hotplate stirrer IKA RCT Digital (0–310°C, 0–1500 rpm), IKA – Werke GmbH & Co. KG, Germany;
- ✓ Magnetic stirrer BOECO MSH-300N (0–310°C, 50–1250 rpm);
- ✓ T60 Visible Spectrophotometer, PG Instruments Limited, UK;
- ✓ Thermostated vertical Franz diffusion cell, 25 mm diameter, acceptor compartment volume 10 mL, Perme Gear, SES GmbH, Germany;
- ✓ Viscotester Thermo Scientific HAAKE Viscotester 550 with HAAKE™ RheoWin™ Measuring and Evaluation Software, Germany;
- ✓ FT-IR Thermo Fischer Nicolet iS50 spectrometer with ATR reflectance accessory;
- ✓ Particle size and zeta potential analyzer – ZetaSizer, serial number MAL 1106241 (Malvern Instruments, UK);
- ✓ Centrifuge BOECO S-8, BOECO GmbH, Germany – for sample volumes above 10 mL;
- ✓ Centrifuge DLAB D2012 Mini Centrifuge, DLAB Scientific Instruments Inc., USA – for sample volumes above 2 mL;
- ✓ HPLC system: Nexera-I LC 2040C 3D plus RF-20A Prominence, fluorescence detector, Shimadzu, Japan;
- ✓ HPLC column: NUCLEODUR®, C18 EC, stainless steel, Int. Ø × L: 4.6 × 250 mm, pore size: 110 Å, particle size: 5 µm, Macherey-Nagel, Agilent Technologies, USA;
- ✓ Clinical centrifuge DLAB DM0412 Low Speed Centrifuge, DLAB Scientific Instruments Inc., USA – for biological samples (blood);

3. Methods

3.1. UV-Vis Spectrophotometric method for quantitative determination of sodium alendronate

For the quantitative determination of NaALD in the preliminary model studies, the UV/Vis spectrophotometric method developed by Kuljanin, J. et al. (2002)[3] was adapted. This

[3] Kuljanin, J. *et al* (2002) 'Spectrophotometric determination of alendronate in pharmaceutical formulations via complex formation with Fe(III) ions', *Journal of Pharmaceutical and Biomedical Analysis*, 28(6), pp. 1215–1220. https://doi.org/10.1016/s0731-7085(02)00021-3

method involves the preparation of a complex between NaALD and Fe(III). The substances react in equimolar ratios in the presence of $HClO_4$. Since NaALD lacks chromophores in its molecule, the formation of a complex with iron ions represents a fast and convenient method of analysis (Kuljanin, J. et al., 2002).

According to the proposed methodology, a stock solution of NaALD (5 mM) in distilled water was prepared, and an equimolar concentration of $FeCl_3$ (5 mM) in 2 M $HClO_4$ (1:1 stoichiometry complex) was added. The absorption spectrum of the resulting solution was studied and compared with the absorption spectrum of $FeCl_3$ solution in $HClO_4$ at various concentrations. A wavelength of λ = 300 nm was selected, since Fe(III) ions exhibit the lowest absorption at this wavelength.

To construct the standard calibration curve, serial dilutions were made from the stock solution in the range of 8.125–325.0 μg/mL. A standard calibration curve was constructed graphically representing the dependence of absorbance on concentration at λ = 300 nm.

3.1.1. Validation

The method was validated with respect to:

Linearity – observed over the concentration range of the analyte where absorbance is linearly dependent on concentration. Linearity was assessed by determining the coefficient of determination (R^2) of the standard line equation obtained from 7 experimental points.

Accuracy – the degree of agreement between the measurement result and the true value of the measured quantity. Determined by spiking a previously analyzed test solution with a known amount of standard stock solution at three levels: 80%, 100%, and 120%.

Precision – shows the variation in values of parallel measurements of the same sample under specified conditions. A quantitative measure of precision is the standard deviation (SD), calculated based on values from n measurements. The method's precision was studied for both intra-day and inter-day variations.

Sensitivity – assessed in terms of the limit of quantification (LOQ) and the limit of detection (LOD) according to ICH Q2(R2) Guideline recommendations. LOQ and LOD were calculated using the following formulas:

$$LOD = \frac{3{,}3 \times \sigma}{S} \quad (1)$$

$$LOQ = \frac{10 \times \sigma}{S}, \quad (2)$$

where "σ" is the standard deviation of the peak areas of the drug (n = 3), and "*S*" is the slope of the corresponding calibration curve.

3.1.2. Influence of polysorbate 80 on the absorption spectra of the ALD/Fe complex

A series of solutions with varying concentrations of polysorbate 80 were prepared in the presence of the functionalizing reagent $FeCl_3$ or the ALD/Fe complex. The UV-Vis spectra of the prepared solutions were recorded and compared to the reference spectra of polysorbate 80, $FeCl_3$, and the ALD/Fe complex. The influence of the hydrophilic surfactant on the absorption spectra of the ALD/Fe complex was evaluated.

3.1.3. Influence of phosphates in the dissolution medium on the formation and absorption spectrum of the ALD/Fe complex

To assess the influence of phosphates in the medium on the formation of the ALD/Fe complex and its absorption spectra, accurately weighed amounts of NaALD were dissolved in SBF 2 mM pH 7.4 (Na_2HPO_4 1.51 mM / NaH_2PO_4 0.49 mM), also containing NaCl 142.0 mM and KCl 5.0 mM. The resulting NaALD concentrations were: 17.7 µg/mL, 28.6 µg/mL, and 35.4 µg/mL. One milliliter of each solution was transferred to 10 mL volumetric flasks functionalized with $FeCl_3$ in 2 M $HClO_4$ and diluted to volume. The absorbance of the ALD/Fe complex at these NaALD concentrations in phosphate buffer was measured in the spectral range of 200 to 400 nm. For comparison, the absorbance of Fe^{3+} in phosphate buffer without NaALD was also measured.

3.2. Solubility of NaALD in lipids and determination of the Water/Oil distribution coefficient (K_{distrb})

To determine the distribution coefficient of NaALD, 10 mL of distilled water were mixed with 1 g of each type of oil (oleic acid, OA; medium chain triglyceride oil, MCT; cod liver oil, CLO; and oleum cocois, OC) using a magnetic stirrer (BOECO MSH-300N) at 250 rpm in a thermostated bath at 70°C. These conditions ensured mutual saturation of the two phases. Then, 10 mg of NaALD was added to each setup and stirred at 250 rpm for 30 minutes. Table 1 presents the model compositions studied.

Table 1. Model Systems: Oil / Water / NaALD

Model 1	Model 2	Model 3	Model 4
10 mg NaALD	10 mg NaALD	10 mg NaALD	10 mg NaALD
1 g Oleic Acid	1 g MCT Oil	1 g Cod Liver Oil	1 g Oleum Cocois
10 mL distilled H_2O	10 mL distilled H_2O	10 mL distilled H_2O	10 mL distilled H_2O
30 min, 250 rpm, 70°C; cooled to 25°C	30 min, 250 rpm, 70°C; cooled to 25°C	30 min, 250 rpm, 70°C; cooled to 25°C	30 min, 250 rpm, 70°C; cooled to 25°C

After 72 hours at room temperature, the samples were centrifuged at 6000 rpm for 30 minutes (BOECO S-8). The aqueous phase was separated, and 2 mL of 0.62M $FeCl_3$/2M $HClO_4$ solution were added. The resulting reaction mixture was diluted with distilled water to 100 mL. The NaALD content in the aqueous phase was determined spectrophotometrically at λ = 300 nm (T60 Visible Spectrophotometer).

The distribution coefficient K_{distrb} was calculated using the equation[4]:

$$K_{distrb} = \frac{Cw}{Coil} \quad (3)$$

The solubility of NaALD in the oil phase (mg/g) was expressed as the difference between the initial amount added and the amount found in the aqueous phase.

3.3. Solubilization of NaALD in surfactants

The solubility of NaALD was investigated in various lipid emulsifiers (Polyoxyethylene 20 sorbitan monooleate, PS; sorbitan monolaurate, SL; sorbitan monooleate, SM; polyoxyethylene 20 sorbitan monolaurate, PL) as follows: 100 mg of NaALD were suspended

[4] Martin, A. (1997) Physical pharmacy: Physical chemical principles in the pharmaceutical sciences. ISBN: 81-7431-001-0.

in 2 mL of each emulsifier: PS, SL, SM, PL. The resulting suspensions were homogenized at 250 rpm using a magnetic stirrer at 70°C for 2 hours, then maintained at 37°C for 48 hours to reach equilibrium. Afterward, the suspensions were centrifuged at 6000 rpm for 30 minutes (BOECO centrifuge S-8). The supernatant was extracted with 2 mL of 0.62M $FeCl_3$/2M $HClO_4$ for 10 minutes. After phase separation, the aqueous phase was collected and filtered through a 0.45 μm filter. The resulting filtrate was diluted to 100 mL with distilled water and analyzed by UV/Vis spectrophotometry at λ = 300 nm (T60 Visible Spectrophotometer) for quantitative determination of NaALD.

3.4. Evaluation of the HLB value of the primary W/O emulsion

To determine the HLB of the primary emulsion (H_2O_{dest}/OC), a series of mixtures with varying surfactant/co-surfactant percentage ratios were prepared to cover the broadest possible range, i.e., within an HLB range of 4 to 9. The oil phase (OC) and aqueous phase were mixed in a 1:1 ratio, while the surfactant content was set at 20% of the oil phase - namely, 5 mL OC, 5 mL H_2O_{dest} and 1 g surfactant/co-surfactant.

The phase inversion technique was employed: under magnetic stirring in a beaker, the oil phase (OC with surfactant/co-surfactant) was added dropwise to H_2O_{dest} at 70°C and 250 rpm. The resulting dispersion was homogenized for 5 minutes and then cooled for another 5 minutes under continuous stirring (750 rpm). The obtained emulsions were transferred into centrifuge tubes and left to stand at 25°C for 24 hours. Subsequently, the emulsions were centrifuged (BOECO Centrifuge S-8) at 6000 rpm for 30 minutes and evaluated visually.

3.5. Pseudoternary Phase Diagrams

To assess the optimal surfactant (S) ratios for self-emulsification, pseudo-ternary phase diagrams were constructed using the water titration method[5].

A primary water-in-oil (w/o) emulsion (PE1) was initially prepared, composed of water, OC, and an emulsifier/co-emulsifier system (HLB 7–7.5). Subsequently, a series of mixtures were prepared by combining PE1 with a selected hydrophilic surfactant at varying weight ratios (9:1, 8:2, 7:3, 6:4, 5:5, 4:6, 3:7, 2:8, 1:9). The mixtures were equilibrated at room temperature (25°C) for 24 h to stabilize their compositions.

Each mixture was then subjected to dropwise titration with distilled water under continuous stirring. The water titration was performed at 25°C with constant agitation (BOECO MSH-300N, 250 rpm). Water was added incrementally (0.100 mL every 2 min), with the total volume ranging from 5% to 95% of the sample. After each addition, the system was visually inspected, and phase transitions were recorded based on the following criteria:

- Opaque/milky appearance – coarse dispersion/emulsion;
- Grayish gel-like phase – transitional liquid crystalline structures;
- Opalescent to transparent dispersion – micro/nanoemulsion formation.

3.6. Evaluation of excipients' effects on the stability of primary emulsion PE1

To evaluate the influence of excipients on the stability of NaALD-containing formulations and to examine their potential to prevent coalescence, flocculation, and sedimentation, a series of model formulations were prepared using gelatin, gum arabic, and whey protein concentrate. The water-in-oil (W/O) emulsifier systems employed consisted of

[5] Khan, A.A. et al.(2013) 'Formulation, optimization and characterization of self nanoemulsifying drug delivery system (SNEDDS) of paclitaxel for solubility enhancement', Nanoscience and Nanotechnology Letters, 5(8), pp. 861–867. https://doi.org/10.1166/nnl.2013.1619.

sorbitan monooleate/polyoxyethylene 20 sorbitan monooleate (SM/PS) and sorbitan monooleate/phosphatidylcholine (SM/PCH).

The formulations were prepared using a standard phase inversion emulsification technique. NaALD was initially dissolved in distilled water to obtain a 5% (w/v) clear aqueous solution. Subsequently, 3% (w/w) whey protein concentrate (WPC 80), 3% powdered gum arabic (AG), and 3% gelatin (G) were sequentially added to aliquots of this solution. The components were dispersed under constant magnetic stirring (500 rpm, IKA RCT, Germany) followed by heating to 65°C to ensure complete homogenization.

Phosphatidylcholine (PCH) was selected as a co-emulsifier for SM in specific ratios designed to achieve a theoretical HLB value between 7.0 and 7.5. The surfactant mixtures were dissolved in an appropriate volume of oil phase under continuous stirring (500 rpm) at 65°C. The oil phase was then incorporated into the aqueous phase using high-shear homogenization (12,000 rpm for 15 min; IKA T25 Ultra Turrax Homogenizer), with the homogenization process continuing until the system reached ambient temperature.

Following 12 hours of equilibration at 25°C, the formulations were subjected to visual stability assessment. Samples demonstrating no visible phase separation were further analyzed by centrifugation (6,000 rpm, BOECO centrifuge S-8) with visual inspection at 2-minute intervals to evaluate their resistance to phase separation under accelerated stress conditions.

3.7. Preparation of model formulations of self double emulsifying drug delivery system (SDEDDS – NaALD)

The model SDEDDS-NaALD formulations were prepared using a two-stage emulsification process (IKA T25 Ultra Turrax Homogenizer, IKA RCT hot plate, Germany) (Figure 1). The first stage involved the preparation of a primary water-in-oil (W/O) emulsion through phase inversion. The second stage consisted of a 24-hour equilibration period for the primary emulsions, followed by the addition of hydrophilic surfactant to the formulations. The compositions of the model formulations are presented in Table 2.

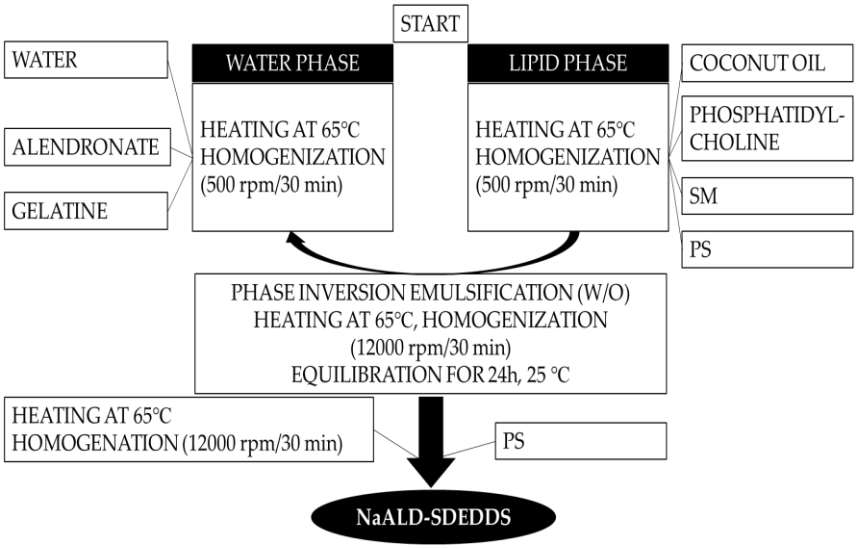

Figure 1: Technological scheme for preparing of the self-emulsifying systems.

Table 2: Composition of SDEDDS-NaALD Formulations: with gelatin (SM/PS), with phosphatidylcholine (SM/PCH), and with both gelatin and phosphatidylcholine (SM/PCH)

Gelatin-containing formulations (SM/PS)					
Formulation, % (т/т)	SMIX1 3.0	SMIX1 3.1	SMIX1 3.2	SMIX1 3.3	SMIX1 „blank”
Alendronate sodium (NaALD)	6,42	6,34	6,22	6,04	-
Gelatine (G)	0,63	1,26	3,12	6,04	-
H_2O_{dest}	18,24	18,12	17.78	17.24	18,34
Phosphatidylcholine (PCH)	-	-	-	-	-
Sorbitan monooleate (SM)	2,96	2,94	2,88	2,80	2,98
Polyoxyethylene 20 sorbitan monooleate (PS)	1,59	1,58	1,55	1,50	1,60
Coconut oil (OC)	18,24	18,12	17.78	17.24	19.61
Polyoxyethylene 20 sorbitan monooleate (PS) – hydrophilic II	51,92	51,64	50.67	49.14	57,47

Phosphatidylcholine-containing Formulations (SM/ PCH)				
Formulation, % (т/т)	PC 2.1	PC 2.2	PC 2.3	PC „blank”
Alendronate sodium (ALDNa)	6,42	6,33	6,23	-
Gelatine (G)	-	-	-	-
H_2O_{dest}	18.36	18.07	17.80	18,34
Phosphatidylcholine (PCH)	1,54	3,04	4,48	2,88
Sorbitan monooleate моноолеат (SM)	3,03	2.99	2.94	1,69
Polyoxyethylene 20 sorbitan monooleate (PS)	-	-	-	-
Coconut oil (OC)	18.36	18.07	17.80	19.61
Polyoxyethylene 20 sorbitan monooleate (PS) – hydrophilic II	52.29	51.50	50.75	57,48

Formulations containing both gelatin and phosphatidylcholine (SM/ PCH)				
Formulation, % (т/т)	PLG 1.1	PLG 1.2	PLG 1.3	PLG 1.4
Alendronate sodium (ALDNa)	6,42	6,17	6,06	5,88
Gelatine (G)	0,63	1,23	3,03	5,88
H_2O_{dest}	18,24	17,64	17,32	16,81
Phosphatidylcholine (PCH)	4,59	4,44	4,36	4,23
Sorbitan monooleate (SM)	2,96	2,61	2,56	2,48
Polyoxyethylene 20 sorbitan monooleate (PS)	-	-	-	-
Coconut oil (OC)	18,24	17,64	17,32	16,81
Polyoxyethylene 20 sorbitan monooleate (PS) – hydrophilic II	48,92	50,27	49,35	47,91

3.8. Thermodynamic stability assessment of SDEDDS-NaALD formulations

Standard solutions were prepared using aqueous emulsions of varying concentrations (v/v). Serial dilutions were performed as follows: 0.1 mL, 0.2 mL, 0.3 mL, 0.4 mL, and 0.5 mL aliquots of the emulsions were diluted with purified water in 50 mL volumetric flasks.

The optical density of the resulting dispersions was analyzed across the visible spectrum. Measurements were conducted using a spectrophotometer (Genesys 10UV, Thermo Scientific, Massachusetts, USA). The absorption spectrum of the highest concentration sample was scanned to determine the wavelength of maximum absorption. All measurements were performed using 1 cm path length cuvettes at λ=230 nm. The equilibrium constant of the process was determined by the dilution method.

Theoretical background for thermodynamic parameter determination

Enthalpy (ΔH), entropy (ΔS), and Gibbs free energy (ΔG) represent fundamental thermodynamic parameters governing system stability. Emulsion stability is influenced by multiple factors including formulation composition, droplet size distribution (colloidal particle dimensions), and other physicochemical characteristics.

The enthalpy change was calculated using the Clausius-Clapeyron equation (4), while entropy and Gibbs free energy were determined through classical thermodynamic equations (5, 6).

$$\frac{d \ln K}{d(1/T)} = \frac{-\Delta H}{R} \tag{4}$$

where ΔH is the enthalpy (kJ mol^{-1}), R is the universal gas constant (R = 8.314 J K^{-1} mol^{-1}), and K is the equilibrium constant.

$$\Delta G = -RT \ln K \tag{5}$$

Entropy is calculated using the classical equation after determining both enthalpy and Gibbs free energy:

$$\Delta S = \frac{(\Delta H - \Delta G)}{T} \tag{6}$$

where ΔS is the entropy (kJ K^{-1} mol^{-1}).

3.9. Self-Emulsification time of SDEDDS-NaALD formulations

The self-emulsification time (SET) was established as the time required for the SDEDDS preconcentrate (equivalent to 35 mg NaALD) to form a homogeneous dispersion upon dilution. The process was monitored visually by observing the development of either an opalescent or clear dispersion.

All experiments were performed in triplicate. The appearance of an opalescent-to-clear dispersion indicated the formation of a micro- or nanoemulsion[6]. A gelatin capsule pre-filled with the model SDEDDS-NaALD formulation was introduced into 200 mL of simulated gastric fluid (pH=1.2, 0.1N HCl) maintained at 37±1°C under gentle agitation (75 rpm, IKA RCT magnetic stirrer, Germany). One-milliliter aliquots of the resulting dispersions were collected for droplet size distribution analysis of the dispersed phase.

[6] Prajapati, S.T., Joshi, H.A. and Patel, C.N. (2012) 'Preparation and characterization of self-microemulsifying drug delivery system of olmesartan medoxomil for bioavailability improvement', Journal of Pharmaceutics, 2013, pp. 1–9. https://doi.org/10.1155/2013/728425

3.10. Assessment of droplet size distribution following SDEDDS-NaALD dispersion

The droplet size (expressed as Z-average) of SDEDDS-NaALD following dispersion (post-self-emulsification) and its size distribution (expressed as the polydispersity index, PDI) were determined using a ZetaSizer (Serial No. MAL 1106241, Malvern Instruments, UK) equipped with a He-Ne laser beam (633 nm) at a fixed scattering angle of 173° and a temperature of 25°C, following the methodology described for self-emulsification time determination. All measurements were performed in triplicate, and results were reported as mean values ± standard deviation (SD) from three independent measurements (n = 3) for each formulation.

3.11. Compatibility assessment

To evaluate the compatibility between components of the selected model formulations, FT-IR analysis was performed[7].

The IR spectra of the model formulations and their individual components were acquired using a Thermo Fisher Nicolet iS50 spectrometer (frequency range: 4000-400 cm^{-1}). The spectra of the raw materials were compared with those of the model formulations.

The spectra of the model formulations were recorded after preparation at 65°C and subsequent storage for 48 hours in hermetically sealed glass vials (25°C, 65% relative humidity).

3.12. Rheological studies

The rheological measurements were conducted at (20±1)°C and (70±1)°C using a Thermo Scientific HAAKE Viscotester 550 (Germany). The analyses were performed with a coaxial cylinder sensor (SV DIN) at shear rates ranging from 0.0123 s^{-1} to 1000 s^{-1}. The shear rate range was selected based on literature references for rheological studies of emulsions containing PS and OC as main components. The total measurement duration was t = 200 s, corresponding to 2 s per measurement point. This measurement time was sufficiently short to prevent structural changes in the emulsions, which can occur during prolonged rheological testing at constant shear rate.

The shear stress data were analyzed as a function of shear rate for each model formulation. Three mathematical models were employed to determine the fundamental rheological parameters presented in Table 3. The mathematical modeling was performed using specialized software integrated with the viscometer.

Table 3: Mathematical Models for Rheological Properties of the Samples

Mathematical models	Mathematical equation
Bingham Plastic Model (BPM)	$\tau = \tau_0 + \eta_p.\gamma$
Power Law Model (PLM)	$\tau = K.\gamma^n$
Herschel-Bulkley Model (HBM)	$\tau = \tau_0 + K.\gamma^n$

Note: τ represents shear stress (Pa), γ denotes shear rate (s^{-1}), τ_0 is the yield stress, K signifies the consistency index ($Pa \cdot s^n$), n corresponds to the flow behavior index, and η_p indicates plastic viscosity.

All measurements were performed in triplicate. The best-fitting model was selected based on the highest coefficient of determination (R^2).

[7] Tabassum, N., Patel, A., Bansal, A.K. and Bhandari, A. (2016) 'Development and evaluation of solid self double emulsifying drug delivery system (SSDEDDS): A novel approach to enhance bioavailability of BCS class III drugs', Journal of Pharmacy Research, 10(6).

3.13. Pharmacopoeial testing of hard gelatin capsules containing SDEDDS-NaALD and In vitro characterization

3.13.1. Uniformity of mass for single-dose preparations

Most commonly, SDEDDS for oral application are formulated in capsules. For the purposes of this study, size "1" hard gelatin capsules (nominal volume 0.5 mL) were filled with model SDEDDS containing a theoretical NaALD content of 32.1 mg (7% w/w). Twenty capsules each of the model SDEDDS formulations PLG 1.1 and Smix1 3.0 were individually weighed to determine both the average mass and individual deviations in accordance with Ph.Eur. 11.0 guidelines.

3.13.2. Uniformity of dosage units

To evaluate the effective drug loading of model SDEDDS-NaALD formulations, dosage unit uniformity testing was performed according to Ph.Eur. 11.0. Ten capsules containing a model SDEDDS were weighed individually. After emptying the contents, the empty shells were reweighed (Method 3.13.1: Uniformity of mass).

The contents of each capsule were dispersed in 1.5 mL of an organic solvent mixture (ethyl acetate/dichloromethane, 3:2 v/v), resulting in the precipitation of a white NaALD residue. The dispersion was subjected to triple extraction with equal volumes of distilled water. The aqueous phases were filtered (0.45 μm) into a volumetric flask and diluted to 100 mL.

A 1 mL aliquot of the resulting solution was transferred to a 10 mL volumetric flask, treated with 1 mL of $FeCl_3/HClO_4$ reagent, and diluted to volume with distilled water. The final solution was analyzed spectrophotometrically at λ=300 nm.

Per Ph.Eur. 11.0 requirements, the NaALD content must fall within ±15% of the theoretical value to comply with the test specifications.

3.13.3. Behavior in biomimetic media

The standard pharmacopoeial dissolution tests demonstrate primary applicability to conventional drug delivery systems (Wolska & Szymańska, 2023)[8] .

Following oral administration under fasted conditions with 200-250 mL of water, the total fluid volume available in the proximal small intestine typically ranges from 300-500 mL[9].

The present study was designed to investigate the behavior of SDEDDS-NaALD in biomimetic media by evaluating both the rate and extent of self-emulsification through determination of the self-emulsification time (SET) and characterization of the system's dispersion properties following emulsification. For this purpose, individual capsules containing either model Smix1 3.0 or model PLG 1.1 were placed in 200 mL of FaSSGF (pH 1.6) and FaSSIF (pH 6.5) media, respectively, the compositions of which are detailed in Table 4.

[8] Wolska, E. and Szymańska, M. (2023) 'Comparison of the in vitro drug release methods for the selection of test conditions to characterize solid lipid microparticles', Pharmaceutics, 15(2), p. 511. https://doi.org/10.3390/pharmaceutics15020511.

[9] Klein S. (2010)The use of biorelevant dissolution media to forecast the in vivo performance of a drug. AAPS J. 2010 Sep;12(3):397-406. doi: 10.1208/s12248-010-9203-3

Table 4: Composition of FaSSGF (pH 1.6) and FaSSIF (pH 6.5) media

FaSSGF pH 1.6		**FaSSIF pH 6.5**	
Sodium taurocholate	80 µM	Sodium taurocholate	3 mM
Lecithin	20 µM	Lecithin	0.75 mM
Pepsin	0.1 $mg.mL^{-1}$	NaH_2PO_4	3.438 g
NaCl	34.2 mM	NaCl	6.186 g
HCl conc.	qs ad pH 1.6	NaOH	qs ad pH 6.5
H_2O_{dest}	ad 1 L	H_2O_{dest}	ad 1 L

The methods employing dialysis membranes and PermeaPad® technology can be adapted to account for the specific properties of drug delivery systems, enabling more precise characterization.

3.13.4. *In vitro* prediction of SDEDDS-NaALD properties

The permeation studies were performed using Franz diffusion cells (Type 3), with the experimental setup illustrated in Figure 2. An 8 mL aliquot of the model SDEDDS-NaALD dispersion in simulated intestinal fluid (FaSSIF, pH 6.5) was introduced into the donor compartment. The receptor compartment (10 mL) contained modified phosphate buffer (Table 5, simulated body fluid adapted from Kokubo and Takadama, 2006) [10]. Two membrane types were employed: a cellulose acetate dialysis membrane (molecular weight cutoff 10,000-14,000 Da) and a biomimetic PermeaPad® Barrier membrane, with an effective diffusion area of 490.87 mm^2.

During the experiments, solution homogeneity was maintained using a Teflon®-coated magnetic stirrer operating at 700 rpm, with temperature controlled at 37±1°C. Samples (500 µL) were withdrawn from the receptor compartment at predetermined time intervals over a 7-hour period for spectrophotometric analysis, with immediate replacement by fresh simulated body fluid to maintain sink conditions. The cumulative percentage of drug released into the receptor medium was plotted as a function of time to establish the permeation profile.

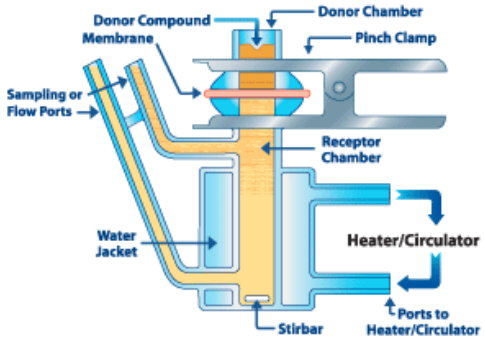

Figure 2: Vertical Franz-type diffusion cell (Type 3), 25 mm in diameter, featuring a 10 mL acceptor compartment.

[10] Kokubo, T. and Takadama, H. (2006) 'How useful is SBF in predicting in vivo bone bioactivity?', Biomaterials, 27(15), pp. 2907–2915. https://doi.org/10.1016/j.biomaterials.2006.01.017

Table 5. Modified simulated body fluid (SBF) composition.

Ions	Plasma (mM)	Modified SBF (mM)
Na^+	142,0	147,44
K^+	5,0	5,0
Mg^{2+}	1,5	-
Ca^{2+}	2,5	-
Cl^-	103,0	147,0
HCO_3^-	27,0	-
HPO_4^{2-}	1,0	1,51
H_2PO^-	-	0,49
SO_4^{2-}	6,5	-

The data obtained from the studies employing both dialysis and biomimetic membranes were utilized to characterize the behavior of the investigated NaALD-containing systems. Regression analysis was performed to identify the model that most accurately describes the permeation kinetics [11].

3.14. Investigation of oral bioavailability of NaALD from SDEDDS through quantification of drug excretion in urine of male Wistar rats

3.14.1. Experimental Animals

The experiments were conducted using male Wistar rats (approximately 100 days old, mean body weight 250 g). The animals were housed in polycarbonate cages with a maximum of six rats per cage under standard laboratory conditions, including an ambient temperature of 22 ± 1°C, a 12-hour light/dark cycle, and free access to food and water following a minimum seven-day acclimatization period.

All animal handling procedures and experimental protocols complied with national regulations (Ordinance No. 20 of 01.11.2012 on the minimal requirements for the protection and humane treatment of laboratory animals and facility standards for their use, breeding, and/or supply), international guidelines (EU Directive 2010/63/EU on animal experimentation), and the ethical standards of the Ethics Committee for Scientific Research at Prof. Dr. Paraskev Stoyanov Medical University, Varna. The study was performed under official authorization for animal experimentation (Permit No. 372 issued by the Bulgarian Food Safety Agency of the Ministry of Agriculture and Food, in accordance with Article 155, Paragraph 7 of the Veterinary Activities Act, and Ethics Committee Opinion No. 288 of 30.11.2023).

[11] Bruschi, M.L., 2015 Strategies to Modify the Drug Release from Pharmaceutical Systems, 1st Edition - June 10, 2015 ,Woodhead Publishing, ISBN: 9780081001127. 9 7 8 - 0 - 0 8 - 1 0 0 1 1 2 - 7.

3.14.2. Analytical method for qualitative and quantitative determination of NaALD in Biological matrices

An adapted analytical methodology was employed based on the procedures described by Han et al. (2012)[12] and Lin et al. (1994)[13]. The direct chromatographic analysis of sodium alendronate presents significant analytical challenges due to its high polarity, absence of suitable chromophores for conventional UV-Vis HPLC detection, and insufficient volatility for gas chromatographic analysis. To overcome these limitations, alendronate can be derivatized at the amino group using specific reagents, thereby enabling reliable chromatographic analysis via HPLC-UV-Vis techniques as previously demonstrated (FABAD, 2006).

Chromatographic separation was performed using a Shimadzu LC-2040C system equipped with an analytical column (250 × 4.6 mm Nucleodur 100 RP18, 5 µm; Macherey-Nagel) and a guard column (40 × 4.6 mm LiChrospher 100 RP18, 5 µm; Merck, Germany). The chromatographic analysis was conducted under the following optimized conditions:

- Mobile phase: acetonitrile:methanol = 1:1 (solution 1) and 12.5 mM citric acid with 12.5 mM sodium pyrophosphate buffer (solution 2) according to gradient program (Table 6);
- Flow rate: 1.1 $mL \cdot min^{-1}$;
- Column temperature: 35°C;
- Injection volume: 50 µL;
- Retention time: alendronate - 7.85 ± 0.30 min and pamidronate - 8.60 ± 0.30 min;
- Detection: fluorescence at λ_{ex} = 260 nm, λ_{em} = 310 nm;

Table 6. Gradient elution program

Time , min	Solution 1, %	Solution 2, %
0 – 22	33	67
22 – 30	68	32
30 – 45	33	67

Sample preparation

Prior to and during the analysis of biological samples, the method was validated over a concentration range of 1–1000 $ng \cdot mL^{-1}$ in accordance with the requirements and principles of Good Laboratory Practice (ICH Q2(R2): Validation of Analytical Procedures (2022). All samples were processed following the proposed method[12].

Alendronate solutions

A stock standard solution of alendronate was prepared in water at a concentration of 1 $mg \cdot mL^{-1}$. Analytical working standard solutions were subsequently obtained by serial dilution of the stock solution with water. Aliquots of 200 µL from these working standards were added to 1 mL of urine, yielding final urinary concentrations of 1, 2, 10, 100, 500, and 1000 $ng \cdot mL^{-1}$. Quality control (QC) samples were prepared similarly at concentrations of 40, 100, and 400 $ng \cdot mL^{-1}$.

[12] Han, H.-K., Shin, H.-J. and Ha, D.H. (2012) 'Improved oral bioavailability of alendronate via the mucoadhesive liposomal delivery system', European Journal of Pharmaceutical Sciences, 46(5), pp. 500–507. https://doi.org/10.1016/j.ejps.2012.04.002

[13] Kang, H., Park, J., Cho, H., Lee, H. and Kim, C. (2006) 'HPLC method validation and pharmacokinetic study of alendronate sodium in human urine with fluorescence detection', Journal of Liquid Chromatography & Related Technologies, 29(11), pp. 1589–1600. https://doi.org/10.1080/10826070600678308.

Pamidronate was employed as the internal standard due to its structural similarity to alendronate (Figure 3).

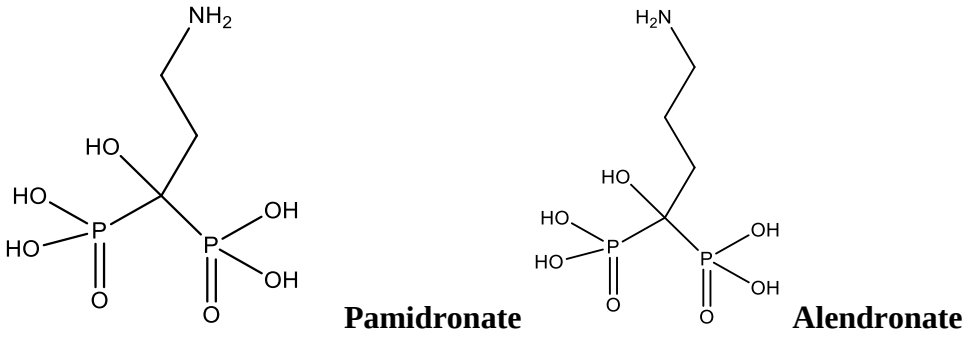

Figure 3. Chemical structures of pamidronate and alendronate.

Solutions of pamidronate (internal standard, IS)

The Panorin® ampoule, containing lyophilized disodium pamidronate, was reconstituted with water to achieve a concentration of 15,000,000 ng·mL^{-1}. Subsequent dilution yielded an internal standard working solution at 10 µg·mL^{-1}. All solutions were stored at 4°C with light protection.

Derivatization of the analyte

To 1 mL of urine sample, 100 µL of internal standard (12,500 ng·mL^{-1} disodium pamidronate) was added, followed by thorough homogenization. Protein precipitation was achieved by adding 3 mL of 6% trichloroacetic acid, and the mixture was centrifuged at 4000 rpm for 10 min. The supernatant was transferred to a fresh tube, and 200 µL of 0.1 M KH_2PO_4, 200 µL of 0.1 M $CaCl_2$, and 400 µL of 1 M NaOH were added. The solution was centrifuged at 3000 rpm for 5 min. The supernatant was aspirated using a vacuum pump, and the remaining pellet was completely dissolved in 500 µL of 0.2 M CH_3COOH, followed by the addition of 3 mL H_2O. The NaOH precipitation step was repeated twice. The final pellet was dissolved in 1 mL of 0.2 M acetate buffer (pH 6.0) and 40 µL CH_3COOH, diluted with 2 mL water. The sample was then loaded onto a DEA SPE cartridge pre-conditioned with 5 mL H_2O. The cartridge was washed twice with 500 µL water, and the drug was eluted with 1 mL of 0.2 M sodium citrate.

For derivatization, 540 µL of the eluate were treated with 200 µL of 1 M sodium carbonate buffer (pH 11.9) and 200 µL of FMOC solution (1 mg in 4 mL acetonitrile). After 5 min, 200 µL of 1 M citric acid were added. Finally, 50 µL of the derivatized sample were injected for analysis.

Preparation of biological calibration standards and quality control samples

For sample preparation, bisphosphonate-free urine was employed as the biological matrix. Prior analysis confirmed the absence of interfering peaks with retention times proximate to those of alendronate and the internal standard, pamidronate. Calibration standards were prepared by adding 200 µL of alendronate working standards and 100 µL of internal standard solution to 1.0 mL aliquots of urine, yielding final concentrations of 1, 2, 10, 100, 500, and 1000 ng·mL^{-1}. Quality control (QC) samples (40, 100, and 400 ng·mL^{-1}) were prepared identically.

The calibration curve was constructed using linear regression analysis of peak area ratios (analyte/internal standard) versus nominal concentrations.

$$y = mx + b \ , \tag{7}$$

where *m* represents the slope of the line and *b* denotes the *y*-intercept. Since the calibration curve is constrained to pass through the origin, the equation simplifies to $y = mx$, where *x* corresponds to the alendronate concentration and *y* is derived from the ratio of the analyte peak area to the internal standard peak area.

Method validation

The methodology was validated for selectivity, sensitivity, accuracy, and precision in accordance with regulatory requirements.

- ✓ Selectivity - the selectivity of the method was demonstrated by comparing chromatograms of calibration standards with those of blank plasma and urine matrices. This confirmed the absence of interfering peaks at the retention times of the analytes.
- ✓ Sensitivity - method sensitivity was determined following ICH Q2(R2) guidelines, with quantification performed at the limit of quantification (LOQ) and limit of detection (LOD).
- ✓ Accuracy and Precision - intra-day and inter-day accuracy and precision were evaluated by analyzing 5 replicates at each concentration level.

3.14.3. Experimental model for evaluation of oral bioavailability of NaALD from SDEDDS via urinary excretion analysis in male Wistar rats

The SDEDDS formulations were adjusted to contain NaALD at a calculated dosage of 5 mg/kg body weight. For animals with an average weight of 250 g, this corresponded to an administered dose of 1.25 mg alendronate contained in 0.5 mL of the model SDEDDS formulation. Control groups received an equivalent volume of placebo vehicle without NaALD.

Animals were distributed into five experimental groups (n=3 per group) as outlined in Table 7, following the *resource equation* method for determining appropriate sample sizes in animal studies [14]. Prior to the experiment, all animals underwent a 24-hour fasting period with ad libitum access to water to standardize metabolic conditions while ensuring proper hydration.

Table 7. Animal group distribution and administered SDEDDS formulation volumes

№	**control group *(+)***		**Placebo PLG 1.1 (-)**		**group PLG 1.1 (+)**		**Placebo Smix1 3.0 (-)**		**group Smix1 3.0 (+)**	
	weight, g	solution, mL	weight, g	SDEDDS, mL	weight, g	SDEDDS mL	weight, g	SDEDDS mL	weight, g	SDEDDS mL
1	260	0,52	220	0,44	250	0,50	260	0,52	200	0,40
2	250	0,50	260	0,52	220	0,44	270	0,54	235	0,47
3	290	0,58	280	0,56	240	0,48	260	0,52	250	0,50

*Positive control: NaALD aqueous solution; Placebo PLG 1.1 (-): PLG 1.1 formulation without NaALD; Group PLG 1.1 (+): PLG 1.1 formulation containing NaALD; Placebo Smix1 3.0 (-): Smix1 3.0 formulation without NaALD; Group Smix1 3.0 (+): Smix1 3.0 formulation containing NaALD.

The collected urine samples were stored in sterile containers at -18°C.

[14] Arifin, W.N. and Zahiruddin, W.M. (2017) 'Sample size calculation in animal studies using resource equation approach', Malaysian Journal of Medical Sciences, 24(5), pp. 101–105. https://doi.org/10.21315/mjms2017.24.5.11

3.15. Statistical Analysis

All experiments were performed in triplicate. The investigated parameters were subjected to statistical analysis, with results expressed as mean values ± standard deviation (SD). Analysis of variance (ANOVA) was employed for comparison of mean values, with a significance level set at $p < 0.05$. Nonlinear modeling was performed using IBM SPSS Statistics 26 (IBM Corp., USA).

Regression analysis to derive models describing the membrane permeation process was conducted using TableCurve™ 2D software (version 5.01, Sigma-Aldrich, St. Louis, MO, USA).

IV. RESULTS AND DISCUSSION

1. UV-Vis Spectrophotometric method for quantitative determination of NaALD

It was adapted a spectrophotometric method for quantitative determination of NaALD Incorporated in the Investigated SDEDDS formulations[3]. The method was validated for four key analytical parameters: linearity, accuracy, precision, and sensitivity.

1.1. Wavelength selection

Equal volumes of standard NaALD and $FeCl_3$ solutions were mixed to assess the absorption characteristics of the ALD/Fe complex. The resulting absorption spectrum was compared with those of individual components: (i) 5mM $FeCl_3$/2M $HClO_4$ and (ii) 5mM NaALD/2M $HClO_4$ (Figure 4). Wavelength selection criteria included:

- Maximum absorption of the ALD/Fe complex
- Minimal interference from Fe^{3+} absorption

Spectral scans (280–400 nm) revealed a λ_{max} of 314 nm for the ALD/Fe complex. Iron ion absorption exhibited near-linear increases between 303–335 nm, with minimal interference observed at 290 nm. Notably, NaALD demonstrated no appreciable absorption across this spectral range. The influence of reactant molar concentration variations on complex absorption was systematically investigated (Figure 5). Increasing molar concentrations of reacting species induced a bathochromic shift of the absorption maximum, while absorbance at 300 nm showed direct proportionality to ALD/Fe complex concentration.

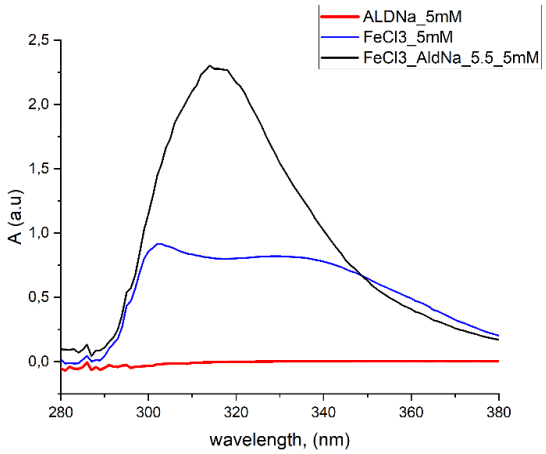

Figure 4. Absorption spectra of NaALD, $FeCl_3$, and the NaALD-$FeCl_3$ complex (ALD/Fe).

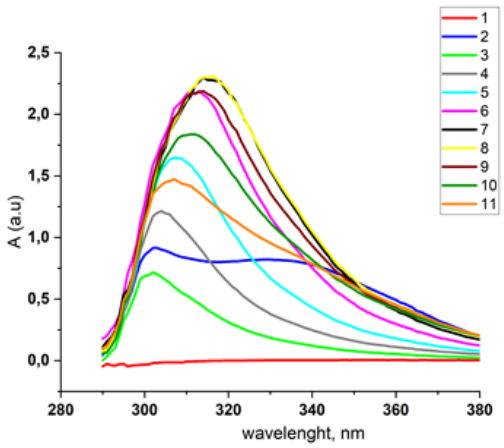

(1) NaALD 5mM; (2) $FeCl_3$ 5mM; (3) $FeCl_3$ /NaALD – 1:9; (4) $FeCl_3$ /NaALD – 2:8; (5) $FeCl_3$ /NaALD – 3:7; (6) $FeCl_3$ /NaALD – 4:6; (7) $FeCl_3$ /NaALD – 5:5; (8) $FeCl_3$ /NaALD – 6:4; (9) $FeCl_3$ /NaALD – 7:3; (10) $FeCl_3$ /NaALD – 8:2; (11) $FeCl_3$ /NaALD – 9:1.

Figure 5. Absorption spectra of the ALD/Fe complex in solutions prepared by mixing $FeCl_3$ and NaALD at varying molar concentrations.

A maximal differential absorption between the formed complex and free Fe(III) was observed at λ = 300 nm, establishing this wavelength as optimal for NaALD quantification. This finding aligns with previous reports by Mabrouk et al. (2018)[15], confirming the analytical validity of the selected wavelength for complexometric determination.

1.2. Validation of UV/Vis Spectrophotometric Method for Quantitative Determination of NaALD

1.2.1. Linearity

The linearity of the method was determined through spectrophotometric measurement of absorption spectra for a series of solutions prepared by appropriate dilutions of $FeCl_3$ (5 mM) in 2M $HClO_4$ and NaALD (5mM) in 2M $HClO_4$ at λ = 300 nm. The concentration range of the ALD/Fe complex spanned 8.125–325.0 µg/mL (Figure 6).

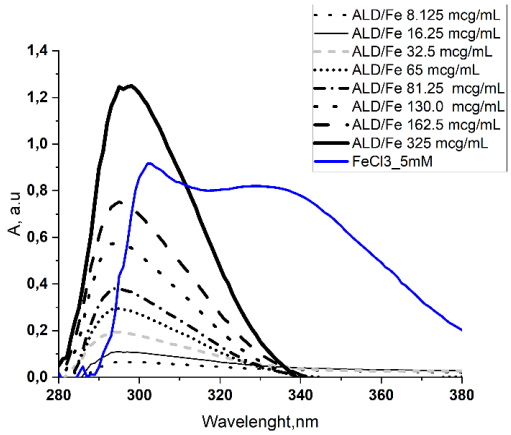

Figure 6. Absorption spectra of the ALD/Fe complex across the concentration range of 8.125–325.0 µg/mL.

[15] Mabrouk, M. et al. (2018) 'Ligand exchange method for determination of mole ratios of relatively weak metal complexes: A comparative study', Chemistry Central Journal, 12(1). https://doi.org/10.1186/s13065-018-0512-4

A standard calibration curve was generated by plotting the absorbance against the concentration of the ALD/Fe complex at λ = 300 nm (Figure 7).

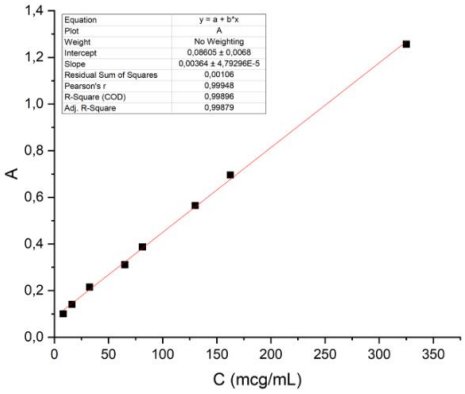

Figure 7. Calibration curve of the ALD/Fe complex at λ = 300 nm.

A linear correlation (R^2 = 0.9989) was established between absorbance and ALD/Fe complex concentration across the range of 8.125–325.0 µg/mL, as represented by Equation 9:

$$y = 0{,}0036x + 0{,}086 \quad (9)$$

1.2.2. Accuracy

The accuracy of the analytical method was evaluated using the standard addition approach. A stock standard solution of NaALD (0.35 mg/mL) was prepared, and a 1 mL aliquot was transferred to a 10 mL volumetric flask. The solution was treated with 1 mL of $FeCl_3/HClO_4$ (5mM) and diluted to volume with distilled water. Absorbance measurements were performed at λ = 300 nm. To pre-analyzed samples (containing 35 µg/mL NaALD), incremental additions of the stock standard solution were made to achieve final spiked concentrations of 28, 35, and 42 µg/mL. Table 8 presents the mean results from triplicate measurements (n = 3) of the solution series.

Table 8. Analytical Recovery Studies (Mean Values from Triplicate Measurements)

Pre-analyzed Sample, (µg/mL)	Added Quantity (µg/mL)	Detected Quantity (µg/mL)	Analytical Recovery, %	RSD, %
35	0	34,4	98,28	1,55
	28	62,68	98,85	0,64
	35	68,41	97,74	1,62
	42	76,94	99,92	0,25

The method demonstrated satisfactory analytical recovery rates ranging from 97.74% to 99.92%, with relative standard deviation (RSD) values below 2%, confirming high accuracy and precision.

1.2.3. Precision

The precision of the method was examined both within-day and in terms of inter-day variations. Table 9 presents the mean values from three measurements.

Table 9: Precision Assessment

Substance	Concentration	Intra-day	Over three separate days

	(µg/mL)	C, µg/mL	RSD, %	C, µg/mL	RSD, %
NaALD	17,5	17,7	1,95	17,4	1,47
	35	36,57	1,55	35,26	1,82
	52,5	51,75	0,77	51,74	0,88

Precision was evaluated by determining the relative standard deviation (RSD%). The data presented in Table 9 demonstrate the method's reproducibility.

The obtained RSD% values were below 2%, confirming that the method is precise with respect to the analyte (per ICH Q2(R2) Guideline).

1.2.4. Sensitivity

The sensitivity of the measurements was expressed as the limit of quantification (LOQ) and limit of detection (LOD). The LOQ and LOD values were calculated according to Equations 1 and 2. The derived values are presented in Table 10.

Table 10: Standard Deviation, LOD, and LOQ

Standart error of the intersept, SE	0,0068
Standart deviation of the intersept, SD	0,0192
LOD	17,637
LOQ	53,445

The derived linear equation (9), y = 0.0036x + 0.086, yielded an LOD of 17.636 µg/mL and an LOQ of 53.445 µg/mL. In addition to selecting an appropriate wavelength, it was necessary to establish the method's application conditions. Since the inclusion of certain excipients in drug delivery systems may interfere with quantitative analysis, their potential influence on the analytical method for NaALD determination was investigated.

1.3. Effect of Polysorbate 80 on the absorption spectra of the ALD/Fe Complex

According to literature data and based on preliminary unpublished in-house studies, certain excipients were found to influence the absorption spectra of the ALD/Fe complex, thereby affecting the quantitative determination of NaALD in the investigated models[16]. Consequently, the impact of polysorbate 80, as hydrophilic emulsifier, on the absorption spectra of the ALD/Fe complex was evaluated in a series of solutions with the following composition:

- $FeCl_3$ 0.37mM solution (in $HClO_4$);
- Polysorbate 80 0.3% solution;
- ALD/Fe complex 0.37mM solution (in $HClO_4$) without polysorbate 80;
- ALD/Fe complex 0.37mM solution (in $HClO_4$) with polysorbate 80 0.3%;
- Fe^{3+} solution 0.37mM (in $HClO_4$) / polysorbate 80 0.3%;
- Fe^{3+} solution 0.37mM (in $HClO_4$) / polysorbate 80 0.6%;
- Fe^{3+} solution 0.37mM (in $HClO_4$) / polysorbate 80 0.9%.

The results are presented in Figures 8 and 9. The influence of polysorbate 80 on the absorption spectra of the ALD/Fe complex in the solution series was significant. The complex's absorption in the range of 290–330 nm remained maximized even at low concentrations. Fe^{3+} ions exhibited low absorption at λ = 300 nm compared to the ALD/Fe complex, which increased substantially in the presence of polysorbate 80. Since the absorption spectrum of polysorbate 80 overlaps with that of the ALD/Fe complex in terms of wavelength, it frequently obscures the signal from the complex.

[16] Wuelfing, W.P., Wang, C.Y., Pan, Y. and Raghavan, K. (2006) 'Polysorbate 80 UV/Vis spectral and chromatographic characteristics – Defining boundary conditions for use of the surfactant in dissolution analysis', Journal of Pharmaceutical and Biomedical Analysis, 41(3), pp. 774–782. https://doi.org/10.1016/j.jpba.2006.01.020

These results demonstrate that the presence of polysorbate 80 in the medium may compromise the applicability of the method. To resolve this issue in the quantitative determination of NaALD in model drug delivery systems (DDS), polysorbate 80 should be removed from the medium prior to measurement, for example, via filtration.

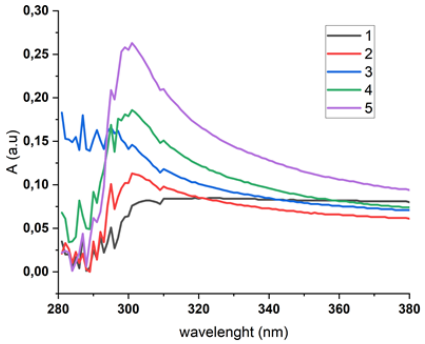

(1) $FeCl_3$ 0,37mM; (2) Polysorbate 80 0,3%; (3) Fe^{3+} 0,37mM /Polysorbate 80 0,3%; (4) Fe^{3+} 0,37mM /Polysorbate 80 0,6%; (5) Fe^{3+} 0,37mM/Polysorbate 80 0,9%;

Figure 8. Absorption spectra of Fe^{3+} in the presence of polysorbate 80.

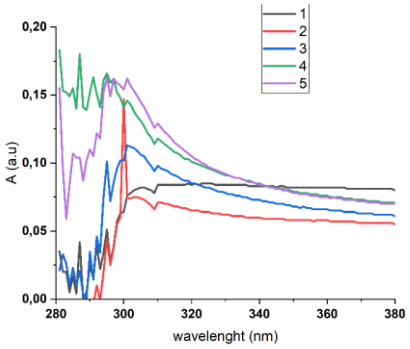

(1) $FeCl_3$ 0,37 mM; (2) ALD/Fe; (3) Polysorbate 80 0,3%; (4) Fe^{3+} 0,37mM/Polysorbate 80 0,3%; (5) ALD/Fe /Polysorbate 80 0,3%;

Figure 9. Absorption spectra of the ALD/Fe complex in the presence of polysorbate80

1.4. Effect of Phosphates in the Dissolution Medium on the Formation of the ALD/Fe Complex and Its Absorption Spectra

Free phosphates in the medium can form compounds with Fe^{3+} ions[17], which in turn may interfere with the quantitative determination of the analyte. The selection of a modified phosphate buffer (SBF) as the medium for predicting NaALD permeation across a membrane in subsequent studies necessitated an evaluation of the influence of phosphates from the SBF[18] medium on the formation of the ALD/Fe complex and its absorption spectra. For this purpose, the absorption spectra of the ALD/Fe complex, prepared at three different NaALD concentrations in SBF, were measured in the spectral range of λ = 200–400 nm. For comparison, the absorption spectrum of Fe^{3+} in phosphate buffer (without NaALD) was used (Figure 10).

[17] Mo, G., Zhao, H., Xu, Y. and Yang, C. (2019) 'Extraction of Fe^{3+} from NaH_2PO_4 solution in a spiral microchannel device', Chemical Engineering and Processing - Process Intensification, 144, p. 107654. https://doi.org/10.1016/j.cep.2019.107654

[18] Zameer, S., Qadir, M.I., Ali, M., Khan, M.S. and Shahzad, Y. (2020) 'Development, optimisation and evaluation of chitosan nanoparticles of alendronate against Alzheimer's disease in intracerebroventricular streptozotocin model for brain delivery', Journal of Drug Targeting, 29(2), pp. 199–216. https://doi.org/10.1080/1061186x.2020.1817041

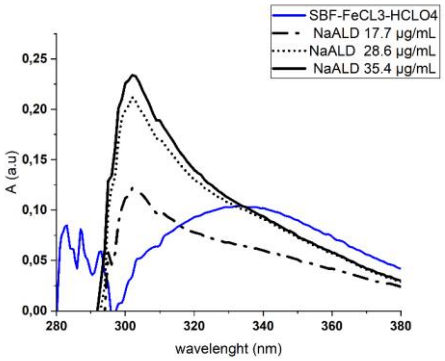

Figure 10: Absorption spectra of NaALD in SBF.

The absorption of Fe^{3+} in SBF at λ = 300 nm is minimal and does not overlap with the absorption maxima of the tested solutions, confirming the method's applicability under the specified conditions.

The selection of excipients is of critical importance for the successful formulation of a stable and functional drug delivery system.

2. Optimization of the SDEDDS composition loaded with NaALD

2.1. Solubility of NaALD in lipids and determination of the water/oil partition coefficient (K_{distr})

Sodium alendronate is highly soluble in water. To predict its behavior in the proposed drug delivery system (DDS), its solubility was investigated in various oils[19]. The experimental conditions and composition of the model oil/water/NaALD systems are detailed in Table 1 (see Materials and Methods). The key difference among the four tested models was the oil phase: oleic acid (Model 1), medium-chain triglycerides (Model 2), cod liver oil (Model 3), and coconut oil (Model 4). These lipids were selected based on their presence in the human diet and their content of absorption enhancers[20]. The water/oil partition coefficient (K_{distr}) of NaALD in these systems was determined using Equation 3. The NaALD concentration in the aqueous phase (C_w) was calculated according to Equation 9, using the mean absorbance value from three consecutive measurements. The NaALD concentration in the oil phase (C_{oil}) was derived as the difference between the initial NaALD quantity and the spectrophotometrically quantified amount in the aqueous phase. Results are presented in Table 11.

Table 11: Water/oil partition coefficient of NaALD in model systems

	Model 1	**Model 2**	**Model 3**	**Model 4**
Loaded amount of NaALD, mg	10	10	10	10
Absorbance (A) at 300 nm	0,383	0,407	0,409	0,363
Determined quantity of NaALD in the aqueous phase (C_w), *mg*	8,260	8,931	8,970	**7,703**
Determined quantity of NaALD in the oil phase (C_{oil}), *mg*	1,740	1,070	1,031	**2,297**
partition coefficient (K_{distr})	4,746	8,355	8,704	**3,354**

[19] Hosny, K.M. (2016) 'Alendronate sodium as enteric coated solid lipid nanoparticles; preparation, optimization, and in vivo evaluation to enhance its oral bioavailability', PLoS ONE, 11(5), p. e0154926. https://doi.org/10.1371/journal.pone.0154926

[20] Nakmode, D. et al (2022). Fundamental Aspects of Lipid-Based Excipients in Lipid-Based Product Development. Pharmaceutics, 14(4), 831. https://doi.org/10.3390/pharmaceutics14040831

Sodium alendronate distributes in the selected oils in the following descending order: CO > OA > CLO > MCT. The superior distribution of NaALD in coconut oil (CO) may be attributed to ionic interactions between the primary amino group of alendronate and the free fatty acids present in coconut oil (European Pharmacopoeia 11.0).Similarly, the solubility of NaALD in these lipids decreases in the same order: CO – 1.15 mg/g, OA – 0.87 mg/g, CLO – 0.54 mg/g, MCT – 0.52 mg/g.

The selection of surfactants and co-surfactants is critical for the system stability. Their stabilizing effects depend on:

- Structural compatibility with the selected lipid and among themselves;
- Their propensity to form stable microemulsions and nanoemulsions;
- Their contribution to the solubilizing capacity of the drug delivery system.

2.2. Solubilization behavior of sodium alendronate in surfactant systems

The solubilization of NaALD in selected surfactants (polysorbate 80 (PS), polysorbate 20 (PL), sorbitan monooleate (SM), and sorbitan monolaurate (SL)) was performed according to the methodology described in the Materials and Methods section. This investigation was necessary to predict drug migration from the internal aqueous phase to the lipid layer. The obtained results are presented in Table 12.

Table 12: Solubilization of NaALD in selected surfactants

Surfactants employed	Concentration of NaALD in the supernatant, mg/mL
SM	2,638
PL	5,617
PS	2,779
SL	4,493

Polysorbate 20 (PL) and sorbitan monolaurate (SL) solubilize 5.6170 mg/mL and 4.4930 mg/mL of NaALD, respectively. These surfactants belong to the polysorbate group and are structurally compatible with coconut oil (CO), as the hydrophobic moiety of both SL and PL molecules consists of lauric acid (monolaurate), while CO contains 40–50% lauric acid.

Although they solubilize a lower quantity and are structurally oleates, the surfactants sorbitan monooleate (SM) and polysorbate 80 (PS) were selected for subsequent studies due to their ability to form more stable emulsions with CO[21]. Furthermore, emulsion stability is also determined by the choice of an optimal emulsifier-to-co-emulsifier ratio.

2.3. Determination of the critical HLB of the primary W/O Emulsion

Based on the results from previous studies (Sections 2.1 and 2.2), model emulsions were prepared. These contained equal ratios of water and coconut oil, along with a two-surfactant system (polysorbate 80, polysorbate 20, sorbitan monooleate, sorbitan monolaurate, or lecithin) with corresponding theoretical HLB values[22]. The compositions of the emulsifier/co-emulsifier systems, as well as the evaluation of the emulsions' physical stability after centrifugation, are presented in Table 13.

[21] Ja'Afar, S. M., Khalid, R. M., Othaman, R., Mokhtar, W.N.A.W. and Ramli, S. (2019); Coconut oil based microemulsion formulations for hair care product application. J. Rheo. Sci. 48(3), 599–605

[22] Schmidts, T., Dobler, D., Nissing, C. and Runkel, F. (2009) 'Influence of hydrophilic surfactants on the properties of multiple W/O/W emulsions', Journal of Colloid and Interface Science, 338(1), pp. 184–192. https://doi.org/10.1016/j.jcis.2009.06.033

Table 13: Emulsifier pair formulations and post-centrifugation stability assessment

HLB	emulsifier 20%	Visual inspection
4,0	SM (100%)	separation
4,4	SM (99,06%) PS (0,94 %)	separation
5,0	SM (93,45%) PS (6,54 %)	separation
6,0	SM (84,11%) PS (15,90%)	no separation
7,0	**SM (74,77%)** **PS (25,23%)**	**no separation**
8,0	SM (65,40%) PS (34,60)	no separation
8,6	SL (100%)	separation
9,0	PCH (100%)	separation

The model emulsions were centrifuged at 6000 rpm for 30 min. All exhibited varying degrees of phase separation, except those with HLB values of 6.0, 7.0, and 8.0. Thus, the range of HLB values yielding stable primary W/O emulsions was visually identified (Figure 11). For subsequent studies, a primary emulsion (PE1) with an HLB of 7.0–7.5 was selected, composed of: water (45.45%), coconut oil (CO, 45.46%), sorbitan monooleate (SM, 6.79%), and polysorbate 80 (PS, 2.29%). According to Rukmini et al. (2012)[23], coconut oil forms stable W/O emulsions within this specified HLB range.

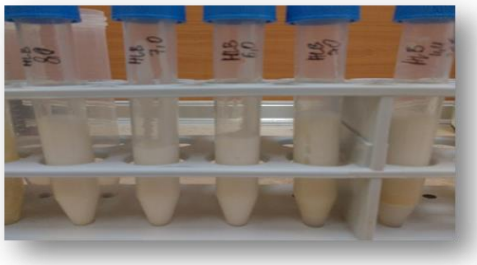

Figure 11: Phase separation behavior of model emulsions post-centrifugation.

For the self-emulsifying drug delivery system (SDEDDS) to form a stable W/O/W emulsion, surfactants must be present in an optimal ratio. Insufficient amounts of hydrophilic surfactant will prevent the formation of a stable multiple emulsion. Conversely, excessively high concentrations may induce toxicity (Maher et al., 2023)[24].

To determine the optimal ratios of components in the emulsion formulation, pseudoternary phase diagrams were constructed.

2.4. Pseudoternary phase diagrams for optimization of hydrophilic emulsifier-to-primary emulsion (PE1) ratio in the SDEDDS formulation

The self-formation of microsized W/O/W double emulsions requires the addition of a secondary (hydrophilic) emulsifier. Polysorbate 80 (PS) was selected based on the results from the studies described in Sections 2.1, 2.2, and 2.3. Pseudoternary phase diagrams were

[23] Rukmini, A., Rahmi, D., & Ibrahim, S. (2012). Formulation and stability testing of water-in-coconut oil emulsions using HLB system. Journal of Pharmaceutical Sciences, 15(3), 112-120

[24] Maher, S. et al (2023) 'Safety of surfactant excipients in oral drug formulations', Advanced Drug Delivery Reviews, 202, p. 115086. https://doi.org/10.1016/j.addr.2023.115086

generated using the methodology outlined in the Materials and Methods chapter. The results are summarized in Figure 12. It was established that the PE1/PS/H_2O (w/w) system forms microemulsions within the following ranges: (5-95)% H_2O and PE1/PS ratios from 1:9 to 4:5. Within the (33.3-50)% H_2O range, with PE1 (11.2-14)% and PS (38.85-51.8)%, a highly viscous gel-like structure was observed (Figure 12).

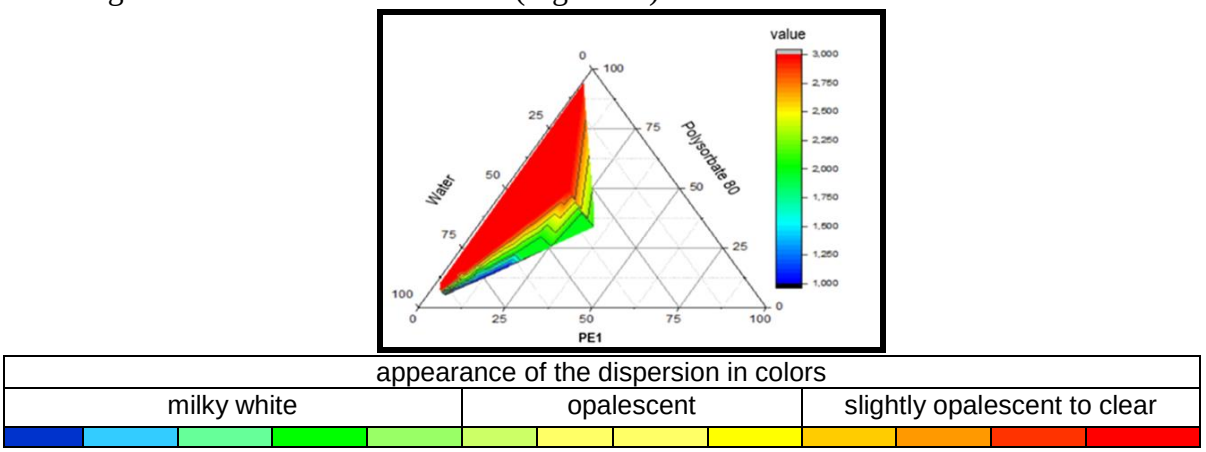

Figure 12: Pseudoternary phase diagram of the PE1/PS/H_2O system, where PE1 is a primary W/O emulsion with an SM/PS surfactant system at a 74.77%/25.23% ratio.

For the formulation of the self-emulsifying system, the minimal required amounts of PS as a secondary emulsifier relative to PE1 ranged between 51% and 54% (v/v).

The internal aqueous phase, which contains the dissolved active pharmaceutical ingredient (API), is dispersed within the oil phase. While the selection of an appropriate emulsifier system is critical, it is not always sufficient to ensure stable emulsion formation[25].

In aqueous solution, NaALD dissociates into alendronate and Na^+ ions (pH 4–5). The iso-osmotic concentration, calculated using Raoult's law for electrolytes, is approximately 5.06% (Equation 10):

$$\Delta T = iK_e\, m, \tag{10}$$

where ΔT is the change in boiling/freezing temperature, K_e is the ebullioscopic constant of the solvent (0.52 °C·kg/mol for water), *m* is molality, and *i* is the ionization coefficient.

Differences in osmolality between the internal and external aqueous phases create a driving force for water migration across the lipid barrier. Changes in the ratio of the internal aqueous phase to the oil phase may compromise physical stability. This can be mitigated by incorporating an osmotically active agent. An alternative approach to limit coalescence of the internal aqueous phase droplets is through gelation[24] .

Model primary emulsions loaded with NaALD (5%) were investigated, along with approaches to stabilize the internal aqueous phase through incorporation of phosphatidylcholine, proteins, hydrocolloids, or polysaccharides (e.g., gelatin, whey protein, gum arabic, etc.)[25,26], as well as combinations thereof.

[25] Oppermann, A.K.L., Moreira, A.L.T., Cavalcanti, R.N. and Hubinger, M.D. (2015) 'Effect of gelation of inner dispersed phase on stability of (W1/O/W2) multiple emulsions', Food Hydrocolloids, 48, pp. 17–26. https://doi.org/10.1016/j.foodhyd.2015.01.027

[26] Devi, L.M., Das, A.B. and Badwaik, L.S. (2023) 'Effect of gelatin and acacia gum on anthocyanin coacervated microcapsules using double emulsion and its characterization', International Journal of Biological Macromolecules, 235, p. 123896. https://doi.org/10.1016/j.ijbiomac.2023.123896

2.5. Investigating the impact of excipients on the stability of the primary emulsion PE1

A series of model water-in-oil (W/O) emulsions containing NaALD in the aqueous phase were prepared (Table 14). The emulsifier systems used were sorbitan monooleate/polyoxyethylene 20 sorbitan monooleate (SM/PS) and sorbitan monooleate/phosphatidylcholine (SM/PCH). The selection of phosphatidylcholine (PCH) was based on literature data supporting its potential to stabilize W/O emulsions containing osmotically active substances dissolved in the internal phase[27]. According to Oppermann et al. (2015)[25], gelation of the internal aqueous phase using whey protein concentrate (WPC 80) or gelatin (G) can enhance emulsion stability and improve the effective encapsulation of active substances in water-in-oil-in-water (W/O/W) emulsions. In line with these findings—and due to their ability to increase viscosity and stabilize the interfacial film—the influence of gum arabic (AG), WPC 80, and G on the stability of the investigated primary emulsions (PEs) was examined (Table 14). The polymer concentration (3%) was selected based on literature reports[25,26,27] .

Following 12 hours of storage at ambient temperature (25°C), the model emulsions incorporating gum arabic (AG) displayed visible phase separation, while those formulated with whey protein concentrate (WPC 80) or gelatin (G) maintained their structural integrity (Figure 13). To further evaluate emulsion stability, the WPC 80- and G-stabilized systems were subjected to analytical centrifugation at 6000 rpm in 2-minute intervals, according to the methodology outlined in Section 3.6.(Materials and methods). The WPC 80 formulations (1) and (2) exhibited significant phase separation after just one centrifugation cycle (Figure 14). In contrast, the gelatin-based systems demonstrated enhanced stability, with the NaALD/G (1) formulation showing phase separation only after three centrifugation cycles, while NaALD/G (2) remained completely stable throughout the testing period.

The experimental results indicate that phosphatidylcholine serves as an effective alternative co-emulsifier to sorbitan monooleate 80 for stabilizing NaALD-loaded W/O emulsions. This phenomenon can be explained by the molecular structure of the phospholipid. The 3-sn-phosphatidylcholine used in this study, being an oleic acid derivative, shares structural similarities with polysorbate 80. This molecular compatibility ensures optimal interaction with both the selected oil phase (composed predominantly of saturated fatty acids) and the sorbitan monooleate 80 emulsifier, thereby contributing to the enhanced stabilization of the emulsion system. The findings align with previous research demonstrating the importance of structural compatibility between emulsifiers and lipid phases in maintaining long-term emulsion stability.

Based on the obtained results, the following conclusions can be drawn:

- **Gelatin has been demonstrated to be suitable for stabilizing the internal aqueous phase of primary emulsions based on both polysorbate 80/sorbitan monooleate 80 (PE1) and phosphatidylcholine/sorbitan monooleate 80 (PE2) systems containing NaALD. However, further research is required to determine the optimal gelatin concentration that would ensure maximum stability of both PE1 and PE2 formulations.**
- **The study has shown that phosphatidylcholine represents a potential alternative to polysorbate 80 as a co-emulsifier with sorbitan monooleate 80 in W/O emulsions. The structural compatibility between phosphatidylcholine and the**

[27] Aniya, N., Peng, Y., Cui, B., Liu, Y. and Guo, J. (2022) 'Improved stabilization and in vitro digestibility of mulberry anthocyanins by double emulsion with pea protein isolate and xanthan gum', Foods, 12(1), p. 151. https://doi.org/10.3390/foods12010151

lipid components of the system contributes to effective emulsion stabilization, suggesting its promising application in similar emulsion formulations.

Table 14: Composition of the primary W/O emulsions

Formulation, % (т/т)	**NaALD / AG (1)**	**NaALD / AG (2)**	**NaALD / WPC 80 (1)**	**NaALD / WPC 80 (2)**	**NaALD / G (1)**	**NaALD / G (2)**
Sodium alendronate (ALDNa)	1.875	1.875	1.875	1.875	1.875	1.875
Coconut oil (OC)	60.00	60.00	60.00	60.00	60.00	60.00
Acacia Gum (AG)	1.125	1.125	-	-	-	-
WPC 80	-	-	1.125	1.125	-	-
Gelatine (G)	-	-	-	-	1.125	1.125
Phosphatidylcholine (PCH)	1.250	-	1.250	-	1.250	-
Sorbitan monooleate (SM)	1.250	1.875	1.250	1.875	1.250	1.875
Polyoxyethylene 20 sorbitan monooleate (PS)	-	0.625	-	0.625	-	0.625
H_2O_{dest}	14.50	29.5	34.995	34.995	34.995	34.995
Observation after 12ч	Phase separation	Phase separation	No Phase separation observed	No Phase separation observed	No Phase separation observed	No Phase separation observed
After cetrifugation	-	-	Phase separation	Phase separation	No Phase separation observed	No Phase separation observed

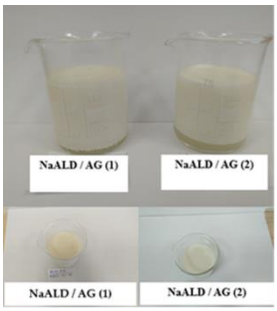

a) NaALD/AG (1) и NaALD/AG (2)

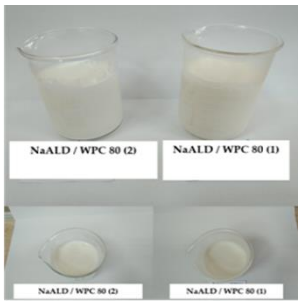

b) NaALD/WPC 80 (1) и NaALD/WPC 80

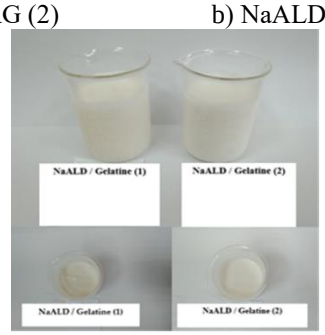

c) NaALD/G (1) и NaALD/G (2)

Figure 13: Model emulsions containing NaALD after 12-hour storage.

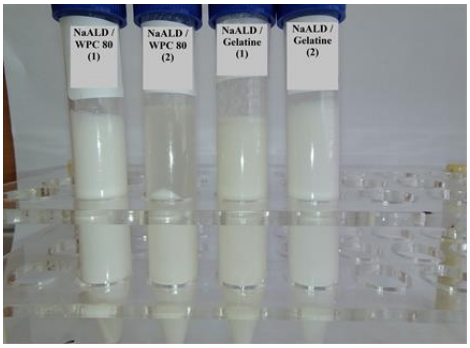

Figure 14: Primary emulsions following analytical centrifugation.

Further investigation is required to examine the self-emulsifying propensity of PE2 when formulated with phosphatidylcholine (PCH) as a co-emulsifier in combination with sorbitan monooleate 80 (SM) and the secondary emulsifier polysorbate 80 (PS).

2.6. Pseudo-ternary phase diagram for determining the secondary emulsifier-to-primary emulsion PE2 ratios

Based on the results presented in Section 2.5, the primary W/O emulsion (PE2) was formulated to consist of water, coconut oil, and an SM/PCH emulsifier system with an approximate HLB of 7-7.5. Visual assessment was performed according to the criteria outlined in Section 2.3 of the "Results and Discussion" chapter. The experimental findings served as the basis for constructing a pseudo-ternary phase diagram (Figure 15).

The PE2/PS/H2O (w/w) system formed microemulsions within the following composition ranges: H2O (5-95)% and PE2/PS ratios from 2:8 to 5:5. In the range of PE2 (2.5-9)%, PS (32-45)%, and H2O (12-25)%, the formation of a viscous, transparent gel-like dispersion was observed. For the development of a self-emulsifying system, the minimal required amounts of PS to be added to PE2 were found to be in the range of (54-56)% (w/w).

As noted in the previous Section 2.5, it is necessary to determine the optimal gelatin concentration in the internal aqueous phase of W/O/W emulsions. To this end, series of model double emulsions were prepared with progressively increasing G concentrations in the internal aqueous phase. For the W/O emulsion systems, both SM/PCH and SM/PS emulsifier pairs were employed in the experimental design.

The systematic investigation of these formulations allowed for the identification of composition ranges that yield stable microemulsion systems while providing insights into the structural transitions occurring at different component ratios. The gel-like phase observed at intermediate compositions suggests the formation of complex interfacial structures that may be advantageous for specific pharmaceutical or cosmetic applications requiring modified release properties. The determination of minimal PS requirements for self-emulsification represents a crucial parameter for the practical implementation of these systems in product development.

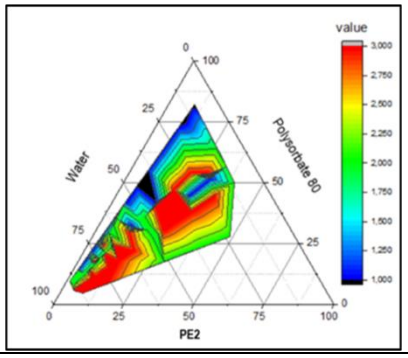

appearance of the dispersion in colors		
milky white	opalescent	slightly opalescent to clear

Figure 15: Pseudo-ternary phase diagram of the W/O emulsion PE2 (SM/PCH system) with polysorbate 80 (PS)

2.7. Model Formulations of W/O/W double emulsions loaded with NaALD

The model W/O/W-NaALD emulsion formulations were prepared using a two-step emulsification technique as described in the Materials and Methods section (Table 2). This procedure yielded homogeneous, gel-like concentrates with an opaque appearance and a characteristic pale yellow-green coloration.

The evaluation of both physical and thermodynamic stability of these model double emulsions is of paramount importance for predicting their *in vivo* behavior, facilitating production scale-up, and determining optimal storage conditions.

2.8. Evaluation of the physical stability of SDEDDS–NaALD via centrifugation

Physical stability was evaluated by analytical centrifugation, performed according to the methodology described in Section 3.6 ("Investigation of the Effect of excipients on the stability of the primary emulsion PE1") of the “Materials and Methods” chapter.

The centrifugation time required for complete phase separation was assessed after each thermal cycle. All model systems exhibited phase separation after one or two centrifugation cycles. The PLG 1.1 and Smix1 3.0 models (Table 2) showed phase separation after 4 centrifugation cycles (Figure 16).

Figure 16: SDEDDS models PLG 1.1 and Smix1 3.0 exhibited phase separation after four cycles of analytical centrifugation.

The 1:10 G/NaALD ratio stabilizes the internal aqueous phase of the model system. The increase in gelatin concentration within the internal aqueous phase (Table 3), regardless of the

W/O emulsifier systems used, leads to an increase in its density. This causes accelerated sedimentation of the system upon application of centrifugal forces[28].

2.9. Thermodynamic stability of SDEDDS–NaALD

The thermodynamic stability was determined by the dilution method, with the equilibrium constant being determined spectrophotometrically[29].The calculated enthalpies of the emulsions exhibited negative values. These results can be associated with exothermic processes[30]. The entropies in the systems showed minimal negative values approaching zero. The results are presented in Table 15.

Model PLG 1.1 is characterized by the highest total Gibbs energy, followed by Smix1 3.0. The Gibbs free energy increased in absolute magnitude in the presence of gelatin and phosphatidylcholine in the emulsion. Consequently, PLG 1.1 is thermodynamically more stable than Smix1 3.0.

Table 15: Thermodynamic parameters of the SDEDDS-NaALD model systems

Модели	ΔG [kJ /mol]	ΔH [kJ /mol]	ΔS [kJ/ mol.K]	K
PLG 1.1	-6,37 ±0,13	-20,11 ±0,39	-005 ±0,01	13,0 ±0,12
Smix1 3.0	-1,91 ±0,07	-18,17 ±0,61	-0,05 ±0,01	2,17 ±0,07

2.10. Compatibility assessment of sodium alendronate with selected excipients in the SDEDDS–NaALD formulation

The recorded FTIR spectra of excipients are presented in Table 16, while those of model formulations appear in Tables 17-18 and Figures 17-18.

In the 3650-3400 cm^{-1} range for both models (Tables 17-18, Figures 17-18), a characteristic band was identified corresponding to terminal -OH groups in polysorbate 80, sorbitan monooleate 80, and system water[31]. No N-H stretching vibrations (~3440 cm^{-1}) characteristic of the aliphatic -NH_2 group in NaALD[32] were observed. Around ~1650 cm^{-1}, both models exhibited a medium-intensity band indicative of hydrogen-bonded, positively charged nitrogen atoms in amino groups.

When the -NH_2 group participates in hydrogen bonding, its characteristic vibrations shift to lower frequencies with reduced intensity, becoming obscured by -OH group signals. The bands at ~2950 cm^{-1}, combined with characteristic amide II absorption bands at ~1470, ~1452, and ~1395 cm^{-1} (Tables 17-18, Figures 17-18), confirm gelatin presence in both formulations. Bands in the ~1750-1730 cm^{-1} (ester C=O) and ~1250 cm^{-1} regions, along with signals at ~2980, ~2920, and ~2850 cm^{-1}, demonstrate aliphatic chains from coconut triglycerides, polysorbate 80, and sorbitan 80.

The PLG 1.1 model spectrum revealed additional bands at ~1452 cm^{-1} (quaternary ammonium) and ~1280 cm^{-1} (phosphate residues) from lecithin/phosphatidylcholine. A weak -OH signal appeared at ~2350 cm^{-1} (Shadmani et al., 2023)[31], absent in Smix1 3.0.

[28] Wankhede, V.P., Sharma, P., Hussain, S.A. and Singh, R.R.B. (2020) 'Structure and stability of W 1/O/W 2 emulsions as influenced by WPC and NaCl in inner aqueous phase. Journal of food science and technology, 57, pp.3482-3492. https://doi.org/10.1007/s13197-020-04383-9

[29] Pokhrel, D.R. et al. (2023) 'A recent overview of surfactant–drug interactions and their importance,' RSC Advances, 13(26), pp. 17685–17704. https://doi.org/10.1039/d3ra02883f.

[30] Gandova, V. and Genov, I. (2020) 'Influence of casein and different supplements into stability of corn oil/water emulsions', Food Science and Applied Biotechnology, 3(1), p. 9. https://doi.org/10.30721/fsab2020.v3.i1.48

[31] Shadmani, N. et al. (2023) 'The synthesis and development of poly (ε-caprolactone) conjugated polyoxyethylene sorbitan oleate-based micelles for curcumin drug release: an in vitro study on breast cancer cells'. RSC advances, 13(34), pp.23449-23460

[32] Ananchenko, G. et al.,(2013) 'Alendronate sodium', Profiles of Drug Substances, Excipients and Related Methodology, 38, pp.1-33. https://doi.org/10.3390/ma15238624

In the fingerprint region, characteristic NaALD bands (C-P-O, PO_3, and P-O-C) appeared at ~1100, ~1070, and ~720 cm^{-1}. PLG 1.1 showed an intense superimposed band at ~1100-1050 cm^{-1} from overlapping phosphate signals of NaALD (~1043 cm^{-1}) and lecithin (~1052 cm^{-1}).

Table 16: FTIR spectra of excipients

No.	Functional group	Band wavenumber (cm^{-1})	
Sodium alendronate			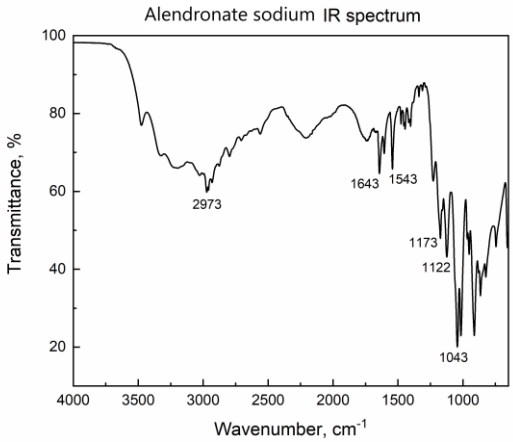
1	-OH, tert	~3500	
2	N-H, amine, str.*	~3440,~1643	
3	C-H, alif, str.	~2973	
4	C-N, amine, str.	~1173, ~1122	
5	C-C str.	~1543	
6	C-H, alcane, str.	~2973, ~ 2958, ~2917	
7	C-P-O PO_3	~1043 ~720	
Coconut oil			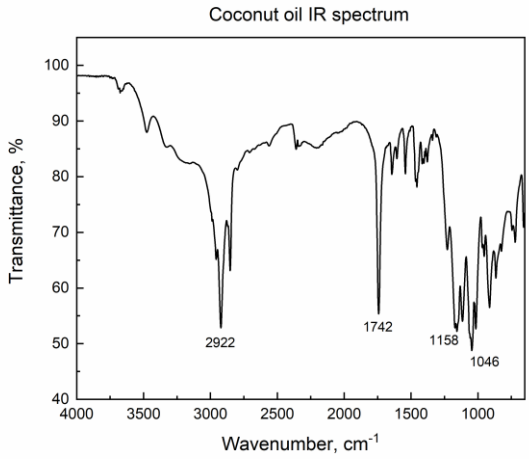
1	C-H, aliphatic chains, $-CH_3$, bend.** $-CH_2$-, bend.	 ~2922 ~2820	
2	C=O, aliphatic acid, str.	~1742	
3	-(C=O)-O-, ester, str.	~1158	
4	-O-CH_2-, aliphatic ester, str.	~1046	
L-α-Lecithin, phosphatidylcholine			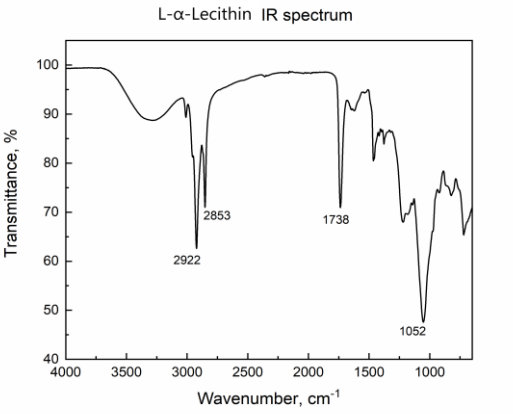
1	$-CH_3$,bend. $-CH_2$-, bend.	~2922 ~2853	
2	-P=O, str.	~1280	
3	-C=O, ester, str.	~1738	
4	$-N^+(CH_3)_3$, str.	~1400	
5	-O-CH_2-, aliphatic, str.	~1100	
6	-P-O-C, str.	~1052	

(*streching, **bending)

Table 16: FTIR spectra of excipients (continued)

No.	Functional group	Band wavenumber (cm^{-1})	
Gelatine			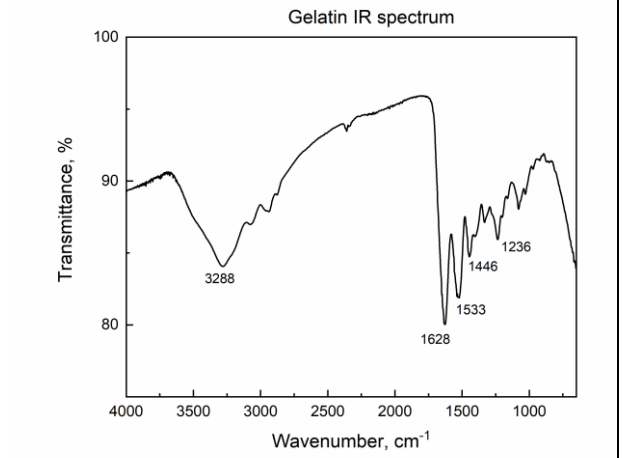
1	-(C=O)-N-, amide A, str.	~3288	
2	-(C=O)-N-, amide I, str.	~1628	
3	-(C=O)-N-, amide II, str.	~1533, ~1521, ~1446	
4	-(C=O)-N-, amide III, str.	~1236, ~1162,~1080,	
5	-C-H, amide, str	~2934	
6	-C-H, proline , str	~1334	
7	-COOH, amide	~1446, ~1334, ~1236	
Sorbitan monooleate 80, SP80			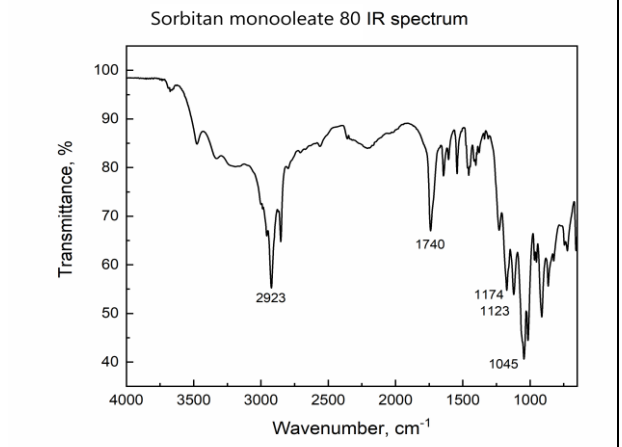
1	-OH , wide, str.	~3399	
2	-C-H, at $-CH_2-$ и $-CH_3$ oaliphatic , str.	~2923 , ~2855	
3	-C=O- , ester , str.	~1740	
4	-C-O, ester, str. O-CH_2-, aliphatic ester, str.	~1174 , ~1123, ~1045	
No.	Functional group	Band wavenumber (cm^{-1})	
Polysorbate 80, TW80			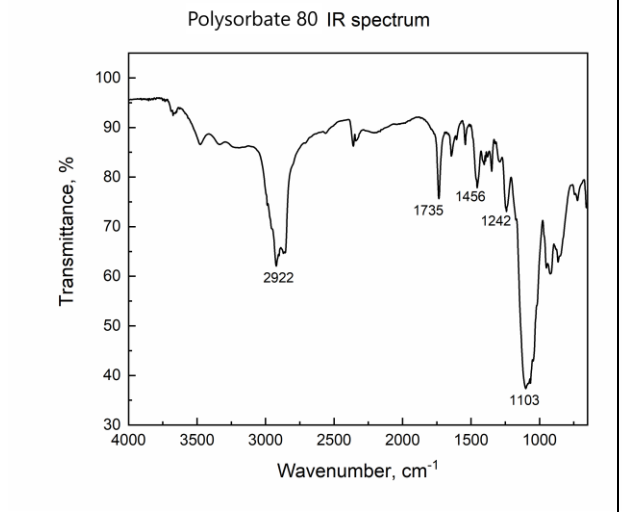
1	-OH , band,str.	~3428	
2	-C-H, при $-CH_2-$ и $-CH_3$ aliphatic, str.	~2922 , ~2912	
3	-C=O-, ester, str.	~1735	
4	-C-O-C, ester, bend.	~1103	
5	C=C, arom. , str.	~1456	
6	C-O-C, str.	~1242	

Table 17: FTIR Spectrum of Model Smix1 3.0

№	Functional group	Band wavenumber (cm^{-1})
1	-OH	~3450
2	-C-H, at $–CH_2$- and $–CH_3$ aliphatic	~2980, ~2920, ~2850
3	-C-H at –CO-NH-	~2950
4	-C=O- , TW80, SP80, fatty acid, aliphatic	~1730
5.	Hydrogen bond	~1650
6	-C=O- , amide II, gelatine	~1470, ~1452, ~1395
7	-C-O, ester, coconut oil	~1250, ~1100
8	-N-C-, amine	~1150
9	C-P-O PO_3	~720 ~1100

Table 18: FTIR spectrum of Model PLG 1.1

№	Functional group	Band wavenumber (cm^{-1})
1	-OH, band	~3450
2	-C-H, at $–CH_2$- and $–CH_3$ aliphatic	~2980, ~2920, ~2850
3	-C-H at –CO-NH-	~2950
4	C-C , cyclic	~2350
5	-C=O- , TW80, SP80, fatty acid, aliphatic	~1730
6	Hydrogen bond	~1650
7	-C=O- , amide II , gelatine	~1470, ~1452, ~1395
8	$-C^{-}O_2$	~1475, ~1440
9	-P=O, ester, lecithine	~1280
10	-N-C-, amine	~1150
11	C-P-O PO_3	~720 ~1100

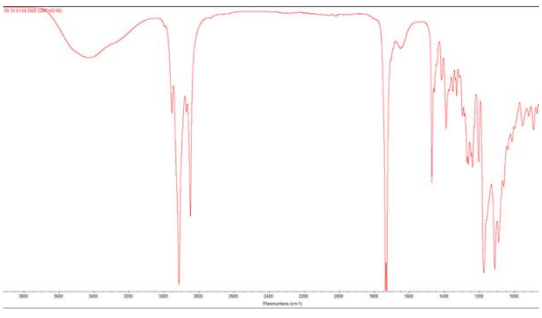

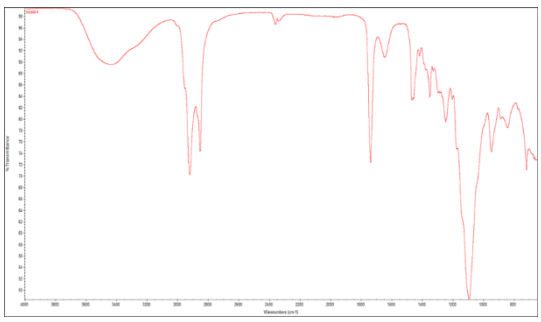

Figure 17:FTIR spectrum of Model Smix1 3.0 **Figure 18:**FTIR spectrum of Model PLG 1.1

The study did not reveal significant changes occurring under the model preparation conditions, confirming the absence of incompatibilities. The presence of hydrogen bonds involving the primary amino group (from alendronate) was detected in the spectra of both models. These findings may partially explain the higher physical stability of the selected model formulations.

SDEDDS should disperse completely and rapidly upon dilution in an aqueous medium with gentle agitation. The self-emulsification time (SET) is a crucial parameter for evaluating emulsion formation efficiency. Ideally, the SET should correspond to the gastric transit time.

2.11. Self-emulsification time (SET) of SDEDDS-NaALD

The self-emulsification time (SET) was determined according to the methodology described in Section 3.9 ("Self-Emulsification Time") of the Materials and Methods chapter (Figure 19).

Under the selected conditions, the SET was 70 min for PLG 1.1 and 69 min for Smix1 3.0. These results are consistent with the average gastric transit time of pharmaceutical formulations under fasting conditions[33]. This finding is supported by the studies of Worsøe et al. (2011)[34], who reported gastric transit times ranging from 56 to 57.5 min.

The slightly opalescent dispersion observed during SET determination (Figure 19) for the SDEDDS-NaALD models confirms the results obtained from the pseudoternary phase diagrams (Figures 12 and 15).

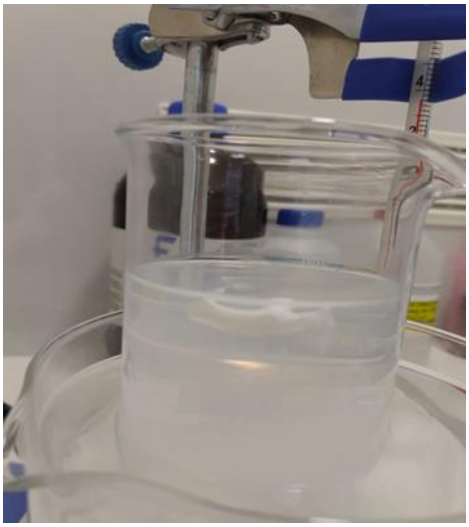

Figure 19: Determination of SET (Self-Emulsification Time)

2.12. Evaluation of dispersed phase droplet size following self-emulsification of SDEDDS-NaALD

Aliquots (1 mL) of the resulting dispersion from the SET determination were analyzed to assess the droplet size distribution of the dispersed phase. According to the obtained results, PLG 1.1 (Figure 20a) and Smix1 3.0 (Figure 20b) self-emulsify into microemulsions. Both models are characterized by a bimodal droplet size distribution. PLG 1.1 shows peaks at 178.4 nm (82.4%) and at 21.47 nm (17.6%), while Smix1 3.0 exhibits peaks at 181.4 nm (54%) and 22.78 nm (46%).

[33] O'Grady, J., Murphy, C.L., Barry, L., Shanahan, F. and Buckley, M. (2020) 'Defining gastrointestinal transit time using video capsule endoscopy: a study of healthy subjects' , Endoscopy international open, 8(03), pp.E396-E400

[34] Worsøe, J., Fynne, L., Gregersen, T., Schlageter, V., Christensen, L.A., Dahlerup, J.F., Rijkhoff, N.J., Laurberg, S. and Krogh, K. (2011) 'Gastric transit and small intestinal transit time and motility assessed by a magnet tracking system', BMC gastroenterology, 11, pp.1-10. https://doi.org/10.1186/1471-230X-11-145

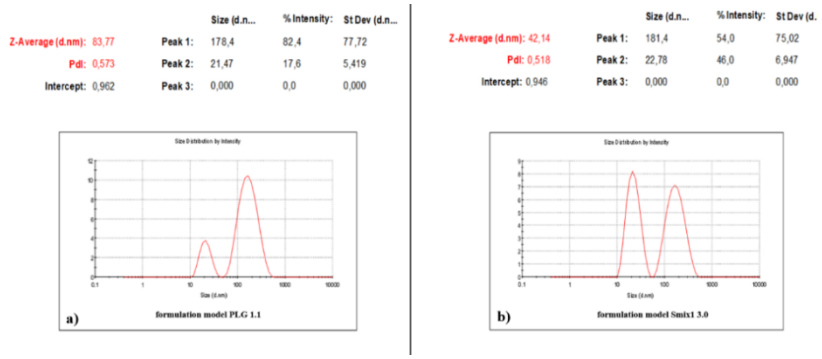

Figure 20: Particle size distribution after self-emulsification of PLG 1.1 (a) and Smix1 3.0 (b).

The rheological properties at different temperatures are fundamental characteristics, both during production and storage. SDEDDS are typically incorporated into soft gelatin capsules at 65-70°C and stored at room temperature.

2.13. Rheological Characterization of SDEDDS–NaALD

The results of the conducted rheological studies demonstrate that the PLG 1.1 and Smix1 3.0 formulations are non-Newtonian fluids exhibiting pseudoplastic behavior at 20°C. Smix1 3.0 displays higher plastic viscosity than PLG 1.1. At 70°C, both PLG 1.1 (Figure 21a) and Smix1 3.0 (Figure 21b) models demonstrate Newtonian fluid behavior. These findings suggest that PLG 1.1 and Smix1 3.0 are suitable for soft capsule filling when formulation stability at elevated temperatures is required[35].

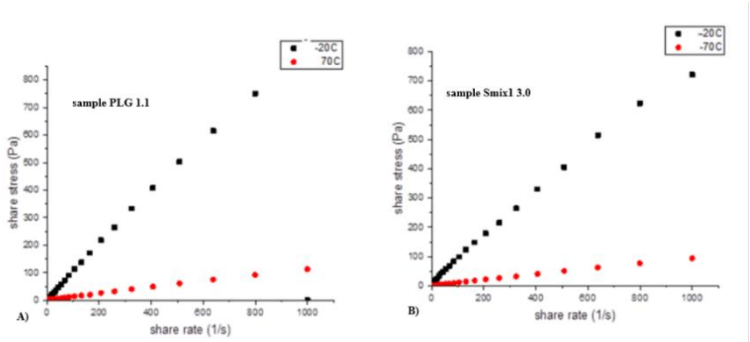

Figure 21: Rheological behavior of SDEDDS-NaALD at 20°C and 70°C: PLG 1.1 (A) and Smix1 3.0 (B).

The most appropriate rheological model describing PLG 1.1 and Smix1 3.0 is the Herschel-Bulkley model. The results from the applied rheological models at 20°C are presented in Table 19. The Herschel-Bulkley model demonstrated the best fit with the experimental data, as evaluated through the coefficient of determination (R^2) and root mean square error (RMSE).

Yield stress determination provides insight into the structural stability of the materials. Below the yield stress, the substance deforms as an elastic solid, while above the yield stress, it flows as a viscous fluid[36]. PLG 1.1 exhibited no yield stress, unlike Smix1 3.0. This observation may be attributed to the presence of soy lecithin in the PLG 1.1 formulation.

[35] Gullapalli, R.P. (2010) 'Soft gelatin capsules (Softgels),' Journal of Pharmaceutical Sciences, 99(10), pp. 4107–4148. https://doi.org/10.1002/jps.22151

[36] Martins, L.S. et al., (2021) 'Properties of cellulose nanofibers extracted from eucalyptus and their emulsifying role in the Oil-In-Water pickering emulsions,' Research Square (Research Square) [Preprint]. https://doi.org/10.21203/rs.3.rs-413307/v1

Similar findings were reported by Bhattacharya et al. (1993)[37], who noted the absence of yield stress in lecithin-stabilized soybean oil emulsions.

Table 19: Rheological parameters of model formulations PLG 1.1 and Smix1 3.0 at 20°C

Sample	Herschel-Bulkey model				
	R^2	RMSE	n	K, Pa.s	τ_0, Pa
PLG 1.1	0,85	0,1084	0,55 ±0,10	11,8 ±1,10	0±0,10
Smix1 3.0	0,999	0,0895	0,89 ±0,10	1,6 ±0,10	1,41±0,10
	Ostwald-Weel model				
PLG 1.1	0,845	0,1084	0,56 ±0,10	10,83 ±0,70	
Smix1 3.0	0,995	0,0895	0,89 ±0,01	1,63 ±0,08	
	Bingham behaviour				
PLG 1.1	0,849	0,1084	0,58 ±0,08		23,72±1,90
Smix1 3.0	0,995	0,0895	0,76 ±0,01		7,63±1,78

3. Technological and biopharmaceutical characterization of SDEDDS-NaALD formulations in hard gelatin capsules

For oral administration, SDEDDS are delivered in capsule dosage form. For the purposes of this study, size "1" gelatin capsules (nominal volume 0.5 mL) were filled with the selected model SDEDDS formulations and underwent technological characterization. Each capsule contained a theoretical NaALD content of 32.1 mg.

3.1. Uniformity of mass of hard gelatin capsules containing SDEDDS-NaALD

Mass uniformity was determined according to the methodology described in the Materials and Methods chapter. The results are presented in Table 20. According to Ph.Eur.11.0 for capsules:

- mass ≤300 mg, the permissible deviation is ±10%;
- mass ≥300 mg, the permissible deviation is ±7.5%.

The mean capsule mass for formulations containing Smix1 3.0 is 0.476 g and PLG 1.1 is 0.447 g .The applicable deviation falls within ±7.5%. The measured average mass of the gelatin shells was 73.5 mg.

Only one capsule, containing Smix1 3.0, exceeded the specified range (0.512–0.440 g) but remained within twice the permissible deviation. All capsules, containing PLG 1.1, complied with the target range (0.481–0.413 g).

[37] Bhattacharya, S., (1993) 'Some physical and engineering properties of tamarind (Tamarindus indica) seed,' Journal of Food Engineering, 18(1), pp. 77–89. https://doi.org/10.1016/0260-8774(93)90076-v

Table 20. Uniformity of mass of hard gelatin capsules containing SDEDDS-NaALD

№	Smix1 3.0 mass/capsule (g)	PLG 1.1 mass/capsule (g)	№	Smix1 3.0 mass/capsule (g)	PLG 1.1 mass/capsule (g)
1	0,464	0,450	11	0,475	0,449
2	0,476	0,447	12	0,475	0,448
3	0,475	0,440	13	0,475	0,440
4	0,488	0,441	14	0,487	0,444
5	0,491	0,466	15	0,489	0,465
6	0,476	0,447	16	0,476	0,447
7	0,475	0,440	17	0,475	0,440
8	0,424*	0,447	18	0,468	0,447
9	0,476	0,450	19	0,476	0,450
10	0,488	0,441	20	0,488	0,441

Both formulations meet the mass uniformity requirements for single-dose preparations.

3.2. Uniformity of dosage units for hard gelatin capsules containing SDEDDS-NaALD

Uniformity of dosage units was determined according to the methodology described in the Materials and Methods chapter. The results are presented in Table 21.

Table 21: Uniformity of dosage units

model SDEDDS	NaALD content in capsules (mg)		
	*Theoretical **	*Found***	*Requirement*
model Smix1 3.0	32,95	32,85	37,89-28,01
model PLG 1.1	31,42	31,30	36,13-26,71

The determined values for both formulations fall within the acceptable deviation limits and thus comply with the test requirements.

The obtained results (Sections 3.1 and 3.2) confirm the conclusions from the rheological studies (Section 2.13). The investigated SDEDDS model formulations demonstrate potential to ensure the production of capsule dosage units with uniform distribution of NaALD dose. Process scaling to industrial production requires additional investigations beyond the scope of this doctoral dissertation.

The biopharmaceutical characterization of model SDEDDS under conditions closely approximating physiological parameters is crucial for predicting their in vivo performance. This serves as a prerequisite for establishing in vitro-in vivo correlation (IVIVC), which can be utilized as: a quality control tool, a means for finished product optimization and a waiver for bioavailability studies.

3.3. Self-emulsification time and dispersity of hard gelatin capsules containing SDEDDS-NaALD in biomimetic media

One capsule each containing model Smix1 3.0 and model PLG 1.1 was placed in 200 mL of FaSSGF (pH 1.6) and FaSSIF (pH 6.5) media, the composition of which is described in the

Materials and Methods chapter. The self-emulsification time (SET) of the models in different biomimetic media was determined (Table 22).

Table 22: Self-emulsification time in biomimetic media

Model	BCE в FaSSGF pH 1,6, (min)	BCE в FaSSIF pH 6,5, (min)
Smix1 3.0	49*	62*
PLG 1.1	80 **	82**

Pale grey opalescent dispersion * , Pale yellow dispersion**

The dispersity of the models in different media was determined. Their intensity- and volume-based polydispersity are presented in Figures 22-25, compared to those of the blank media.

Analysis of the FaSSGF (pH 1.6) medium for intensity distribution showed a peak at 596.8 nm with Z-average of 675.2 nm and PDI of 1.0 (Figure 22). The volume distribution of the same FaSSGF (pH 1.6) medium was again characterized by a single main peak at 559.8 nm with z-average of 675.2 nm (Figure 23). This result may be explained by the formation of aggregates and micelles from the lecithin and taurocholate[38] contained in the medium (Figure 22). The observed aggregates represent a broadly dispersed population, as evident from the PDI value of 1.0 [39].

The analysis of the dispersity of the models in the same medium (FaSSGF, pH 1.6) shows the following results (Figures 22 and 23):

• Model Smix1 3.0: The intensity measurement reveals a bimodal distribution with peaks at 156 nm (74.71%) and 21.77 nm (25.29%), z-average 63.13 nm and PDI 0.553 (Figure 22). The volume distribution also shows a bimodal distribution with two main peaks at 136.5 nm (2.29%) and 18.48 nm (97.7%) (Figure 23).

• Model PLG 1.1: A bimodal distribution is observed with two main peaks in intensity at 373.9 nm (50.67%) and 19.99 nm (49.33%), with z-average 199.1 nm and PDI 0.406 (Figure 22). The analysis of the volume distribution shows one main peak at 16 nm (99.39%) and one secondary peak at 388.2 nm (0.61%) (Figure 23).

[38] Naso, J.N. et al . (2019) 'Studies on the interactions between bile salts and food emulsifiers under in vitro duodenal digestion conditions to evaluate their bile salt binding potential', Colloids and Surfaces B: Biointerfaces, 174, pp.493-500. https://doi.org/10.1016/j.colsurfb.2018.11.024

[39] Nobbmann, U. (2017) Polydispersity – What does it mean for DLS and chromatography? Available at: https://www.malvernpanalytical.com/en/learn/knowledge-center/insights/polydispersity-what-does-it-mean-for-dls-and-chromatography

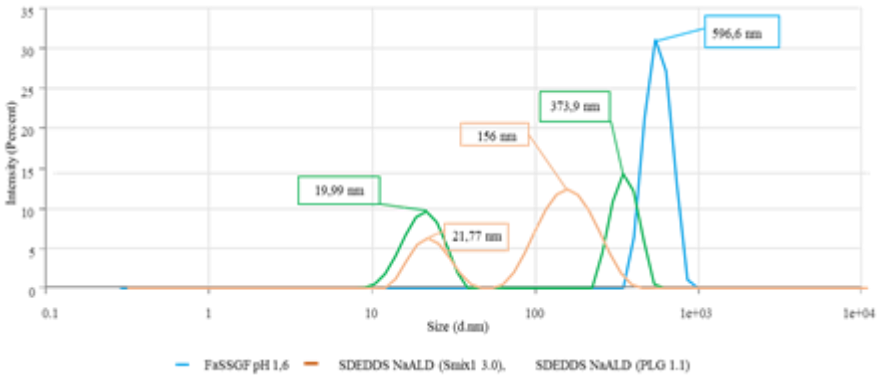

Intensity distribution	Z-Average, (nm)	PDI	Intercept	Peak 1		Peak 2	
				nm	%	nm	%
FaSSGF pH 1,6	675,2	1	0,7276	596,6	100,0	-	-
SDEDDS ALDNa (Smix1 3.0)	63,13	0,553	0,7678	156	74,71	21,77	25,29
SDEDDS ALDNa (PLG 1.1)	199,1	0,4064	0,9318	373,9	50,67	19,99	49,33

Figure 22: Comparative analysis of intensity-based size distribution of Smix1 3.0 and PLG 1.1 in FaSSGF medium (pH 1.6).

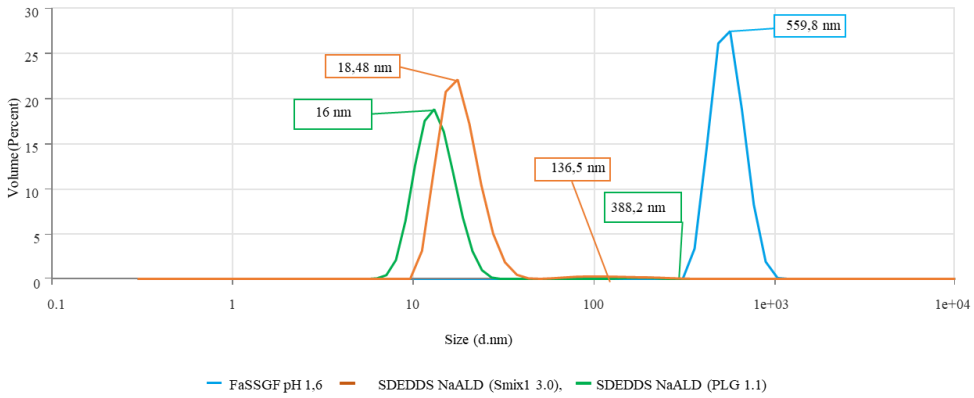

Volume distribution	Z-Average, (nm)	Standart Deviation SD	Peak 1		Peak 2	
			nm	%	nm	%
FaSSGF pH 1,6	675,2	-	559,8	100	-	-
SDEDDS ALDNa (Smix1 3.0)	63,13	0,5378	136,5	2,296	**18,48**	**97,70**
SDEDDS ALDNa (PLG 1.1)	199,1	0,5378	388,2	0,61	**16,00**	**97,46**

Figure 23: Comparative analysis of volume-based size distribution of Smix1 3.0 and PLG 1.1 in FaSSGF medium (pH 1.6).

The comparative analysis of the dispersity of the two models shows the absence of the peak characteristic of the FaSSGF medium (pH 1.6). This indicates that the components of the medium influence the process and degree of self-emulsification. In the volume-based distribution analysis, the observed peaks at 18.48 nm (model Smix1 3.0) and 16.00 nm (PLG 1.1) (Figure 23) are indicative of microsized emulsion formation. The determined droplet sizes of the predominant population in the dispersed phase in both cases can be explained by

the significant amount of hydrophilic surfactant (over 30%), and the process is partially facilitated by the presence of small amounts of NaCl, taurocholate, and lecithin in the medium[40].

Similarly, the behavior of the model SDEDDS was investigated in the biomimetic FaSSIF medium at pH 6.5, since NaALD is primarily absorbed in the duodenum and proximal part of the small intestine. The behavior of the model systems in biomimetic media is of essential importance for predicting their *in vivo* performance.

The analysis of the medium for intensity-based distribution shows a bimodal distribution with peaks at 275.3 nm (94.87%) and 4705 nm (5.13%), with a z-average of 240.9 nm and narrow polydispersity (PDI 0.3214) (Figure 24). The volume-based distribution is also bimodal, with peaks at 314.4 nm (85.96%) and 4892 nm (14.04%) (Figure 25). These results correspond with the higher concentrations of lecithin and bile salts.

One capsule each containing model Smix1 3.0 and model PLG 1.1 was placed in 200 mL FaSSIF (pH 6.5). After obtaining a homogeneous dispersion, the analyzed aliquots showed the following results (Figures 24 and 25):

• Model Smix1 3.0: A multimodal intensity-based distribution was observed with peaks at 335.4 nm (95.96%), 4937 nm (2.174%), and 12.96 nm (2.134%), with a z-average of 177.1 nm and PDI 0.5155, indicating broader polydispersity. The volume-based distribution was also multimodal, characterized by peaks at 601.9 nm (6.705%), 5071 nm (0.4239%), and 15.58 nm (92.87%).

• Model PLG 1.1: The intensity-based distribution was multimodal with peaks at 407.9 nm (56.28%), 18.45 nm (22.31%), and 91.48 nm (21.41%), with a z-average of 365.7 nm and PDI 0.4485, indicating moderate polydispersity. The volume-based distribution was again multimodal, characterized by peaks at 424 nm (1.174%), 16.36 nm (97.81%), and 81.45 nm (1.016%).

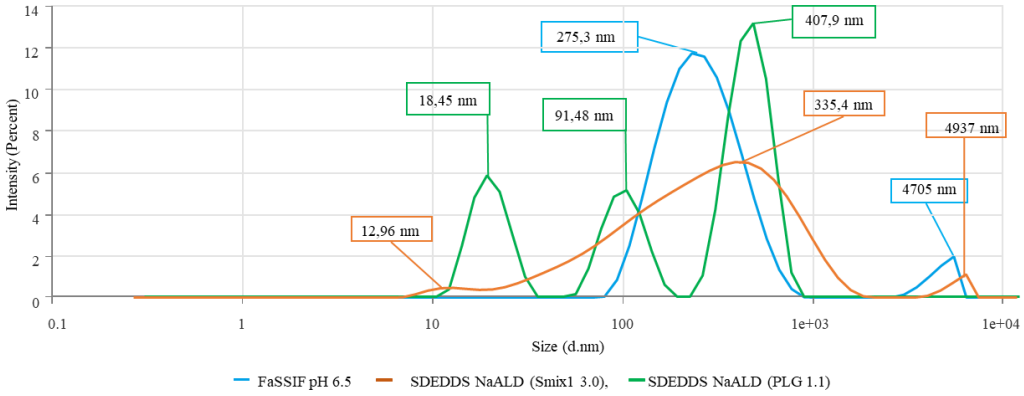

Intensity distribution	Z-Average, (nm)	PDI	Intercept	Peak 1		Peak 2		Peak 3	
				nm	%	nm	%	nm	%
FaSSIF pH 6,5	240,9	0,3214	0,9666	275,3	94,87	4705	5,13	-	-
SDEDDS Na ALD (Smix1 3.0)	177,1	0.5155	0.9761	335,4	95,69	4937	2,174	12,96	2,134
SDEDDS NaALD (PLG 1.1)	365.7	0.4485	0.8949	407,9	56.28	18.45	22.31	91.48	21.41

Figure 24: Comparative analysis of intensity-based particle size distribution of Smix1 3.0 and PLG 1.1 in FaSSIF medium (pH 6.5).

[40] Omarova, M., Swientoniewski, L. T., Mkam Tsengam, I. K., Blake, D. A., John, V., McCormick, A., et al. (2019). Biofilm Formation by Hydrocarbon-Degrading Marine Bacteria and Its Effects on Oil Dispersion. ACS Sustainable Chem. Eng., 7(17), 14490–14499.

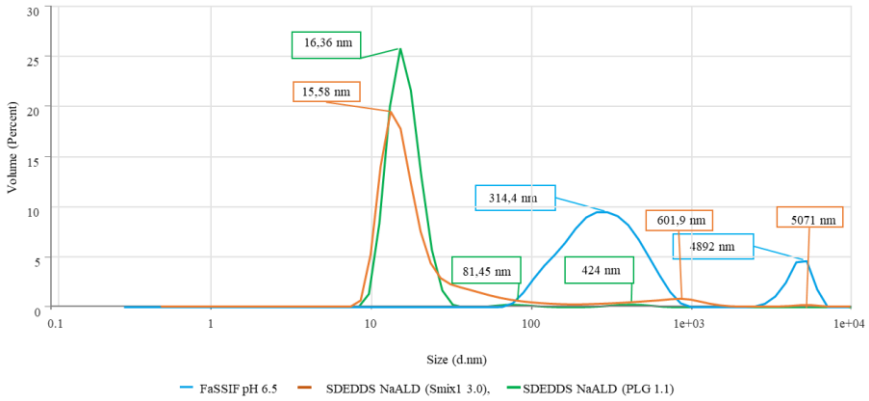

Volume distribution	Z-Average, (nm)	Standart Deviation SD	Peak 1 nm	Peak 1 %	Peak 2 nm	Peak 2 %	Peak 3 nm	Peak 3 %
FaSSIF pH 6,5	240,9	24,24	314,42	85,96	4892	14,04	-	-
SDEDDS NaALD (Smix1 3.0)	177,1	199,6	601,9	6,705	5071	0,4239	**15,58**	**92,87**
SDEDDS Na ALD (PLG 1.1)	365,7	275,8	424	1.174	**16,36**	**97,81**	81,45	1,016

Figure 25: Comparative analysis of volume-based particle size distribution of Smix1 3.0 and PLG 1.1 in FaSSIF medium (pH 6.5).

The comparative analysis of the intensity-based distribution of model Smix1 3.0 shows the presence of a peak (4937 nm) characteristic of the FaSSIF (pH 6.5) medium in the dispersed phase, while this peak is absent in model PLG 1.1. The same volume-based distribution analysis reveals aggregates with medium-specific sizes of 5071 nm again only in model Smix1 3.0. These large aggregates are inherent to the lecithin present in the biomimetic medium. Model Smix1 3.0 (Z-Average 177.1 nm) forms a dispersed phase with smaller sizes than PLG 1.1 (Z-Average 365.7 nm) in both comparative analyses. The volume distribution analysis clearly shows that both models are predominantly composed of microemulsion-sized droplets (92.87% and 97.81%, respectively) (Figure 25).

The change in dispersed phase size for model PLG 1.1 may be explained by the higher concentrations of bile salts and lecithin in the medium, which additionally influence the self-emulsification process. According to A. Torcello-Gómez et al. (2012)[41], bile salts can significantly affect emulsion stability depending on their composition. The process is characterized by adsorption at the interphase surface and penetration into the bilayer by emulsifiers and co-emulsifiers, droplet volume expansion and subsequent droplet breakdown. Model PLG 1.1 contains phosphatidylcholine as a co-emulsifier, which as a zwitterionic surfactant may promote taurocholate adsorption at the oil-water interface. Conversely, the process is hindered by the presence of nonionic surfactants like polysorbate 80, as they are resistant to the influence of bile salts.

The results demonstrate that biomimetic media significantly influence the dispersity of the model systems. Furthermore, it can be predicted that depending on in vivo environmental conditions, the model systems (Smix1 3.0 and PLG 1.1) will initially self-

[41] Torcello-Gómez, A. and Foster, T.J. (2014) 'Interactions between cellulose ethers and a bile salt in the control of lipid digestion of lipid-based systems', Carbohydrate polymers, 113, pp.53-61, https://doi.org/10.1016/j.carbpol.2014.06.070

emulsify into microemulsions, followed by varying degrees of transition to nanoemulsions.

Nanoemulsions (20–500 nm) are thermodynamically unstable but kinetically stable systems. Therefore, it is essential to determine the rate and extent to which SDEDDS will cross epithelial membranes.

Conventional pharmacopeial dissolution tests are primarily applicable to traditional drug delivery systems (DDS)[42]. Methods utilizing dialysis membranes and PermeaPad® membranes can be adapted according to the specific characteristics of the DDS to enable more accurate characterization**.**

3.4. In vitro prediction of NaALD permeation from hard gelatin capsules containing SDEDDS-NaALD

3.4.1. Diffusion through a dialysis membrane

Figure 26 shows the plots depicting the dependence of released NaALD (%) in the medium as a function of time. The hydrodynamic conditions in both the donor and acceptor compartments of the diffusion cell were 70 rpm and T = (37±1)°C. The concentration of released NaALD from the reference dispersion increased most rapidly, followed by Smix1 3.0 and PLG 1.1. All models exhibited a characteristic lag-time (tlag). The results suggest that NaALD diffuses freely along the concentration gradient.

For the model SDEDDS, a retention effect was observed (Smix1 3.0 tlag ~120 min and PLG 1.1 tlag ~240 min), which may be explained by the need for NaALD to first diffuse through the lipid layer of the emulsions. The differences in retention times could be attributed to varying densities of the outer lipophilic layer in the respective model SDEDDS[43]. The presence of a short lag-time in the reference dispersion profile (NaALD 70mg tlag ~60 min) might be due to deposition of taurocholate micelles or other medium components on the dialysis membrane.

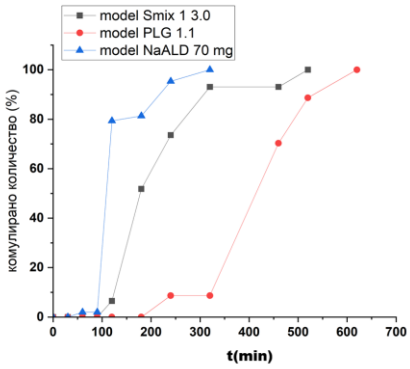

Figure 26: Release profiles of SDEDDS-NaALD models through a dialysis membrane

3.4.2. Diffusion through PermeaPad® biomimetic membrane

Figure 27 shows the plots of released NaALD (%) in the medium as a function of time. The PermeaPad® consists of a phospholipid layer on a porous polymer support. In this

[42] Wolska, E. and Szymańska, M. (2023) 'Comparison of the in vitro drug release methods for the selection of test conditions to characterize solid lipid microparticles', Pharmaceutics, 15(2), p. 511. https://doi.org/10.3390/pharmaceutics15020511

[43] Kalosakas, G. and Panagopoulou, E. (2022) 'Lag time in Diffusion-Controlled release formulations containing a Drug-Free outer layer,' Processes, 10(12), p. 2592. https://doi.org/10.3390/pr10122592

experiment, the dialysis membrane was replaced with a PermeaPad® membrane while maintaining all other conditions.

The phospholipid layer exhibits a "blocking" effect on NaALD permeation, which normally crosses hydrophilic barriers freely. A similarity was observed in the shape of the cumulative curves for both model SDEDDS-NaALD formulations. This similarity, along with differences in lag times, is associated with the influence of excipients in the emulsion compositions.

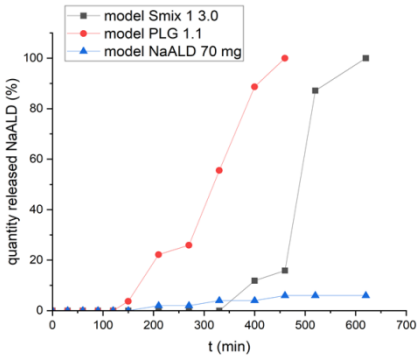

Figure 27: Release profiles of SDEDDS-NaALD models through PermeaPad® membrane

The presence of lecithin in the PLG 1.1 formulation is likely responsible for the shorter *lag time* observed in the concentration increase of NaALD in the acceptor compartment.

Both model SDEDDS formulations achieved nearly complete permeation of NaALD under near-physiological conditions. For model PLG 1.1, approximately 88% of the initial NaALD quantity (t=0) in the donor compartment was released within 5 hours, while model Smix1 3.0 released the same amount of NaALD after approximately 9 hours. The reference model showed only about 5.96% of NaALD transferred to the acceptor compartment after 7 hours.

For more detailed characterization of the NaALD release mechanism from the model SDEDDS and their influence on the drug's membrane permeation capability, the in vitro study data were fitted to fundamental kinetic models: first-order kinetics, Higuchi model, and Korsmeyer-Peppas model. The results are presented in Table 23.

For all evaluated models using the PermeaPad® membrane, the Korsmeyer-Peppas model was most suitable for describing the release process, as evidenced by the determination coefficient R^2 shown in Table 23.

The release from SDEDDS Smix1 3.0, studied using a diffusion model with dialysis membrane, was described by first-order kinetics with R^2=0.958, while SDEDDS PLG 1.1 again followed the Korsmeyer-Peppas model with determination coefficients above 0.9.

The excipients lecithin and polysorbate 80 play a crucial role in enhancing the membrane permeation capability of highly hydrophilic drugs such as NaALD. Model PLG 1.1 demonstrates a superior release profile compared to Smix1 3.0 in in vitro testing, making it a potentially more suitable candidate for in vivo application. According to the proposed Korsmeyer-Peppas kinetic model, the release process and subsequent membrane diffusion are primarily dependent on the "erosion" of the outer lipid layer ($n \geq 0.89$)[44].

[44] Klimashevich, V.B., Kazyuchits, O.A, Zhebentyaev , A.I., Gudovich, V.V., Nasennikova, E.E. (2019) 'Technological aspects of the pharmaceutical development of the ranolazine-based drug,' Vestnik of Vitebsk State Medical University, 18(4), pp. 98–112. https://doi.org/10.22263/2312-4156.2019.4.98

Table 23: Parameters of different mathematical models used to simulate the release and membrane permeation processes

Higuchi model – dialysis membrane			
	K, mg/min		**R^2**
Smix1 3.0	4,2172±0,613		0,621
PLG 1.1	неприложим		n/a
NaALD	5,2090±0,0956		0,557
Higuchi model – PermeaPad® membrane			
Smix1 3.0	2,5270 ± 0,9320		0,1900
PLG 1.1	3,2599 ± 0,2319		0,4601
NaALD	0,2125± 0,0009		0,5928
Korsmeyers'-Peppas – dialysis membrane			
	K, min^{-1}	**n**	**R^2**
Smix1 3.0	0,5180± 0,0060	0,8680 ± 0,0325	0,748
PLG 1.1	$1,67.10^{-10} \pm 0,9.10^{-11}$	4,3631 ± 1,2830	0,9790
NaALD	0,5020± 0,1370	0,9407 ± 0,0414	0,695
Korsmeyers'-Peppas – PermeaPad® membrane			
Smix1 3.0	$5,868.10^{-9} \pm 0,9.10^{-10}$	3,6754± 0,0425	0,767
PLG 1.1	0,0023± 0,0001	1,7578± 0,0220	0,9005
NaALD	0,0013± 0,0001	1,3694± 0,184	0,9586
First order kinetics model - dialysis membrane			
	K, min^{-1}	**$logC_0$**	**R^2**
Smix1 3.0	0,0088± 0,0004	4,462± 0,1330	0,958
PLG 1.1	0,214 ± 0,0003	3,1380 ± 0,0133	0,4515
NaALD	0,0035± 0,0014	0,6465± 0,235	0,5810
First order kinetics model – PermeaPad® membrane			
Smix1 3.0	0,01656± 0,0001	$5,486.10^{-7} \pm 0,9.10^{-8}$	0,767
PLG 1.1	0,02134± 0,0003	0,8360± 0,0024	0,7738
NaALD	n/a	n/a	n/a

To confirm this hypothesis, the models must be tested in vivo, as in vitro methods are not perfect and do not fully reflect the actual physiology of organisms.

4. Investigation of the oral bioavailability of NaALD from SDEDDS by quantifying drug excretion in urine of male Wistar rats

4.1. Validation of an HPLC-UV/Vis analytical method for quantification of NaALD in biological matrices

The calibration curve was constructed using linear regression according to the methodology described in the Materials and Methods chapter (Figure 28). The method was validated for selectivity, sensitivity, accuracy, and precision.

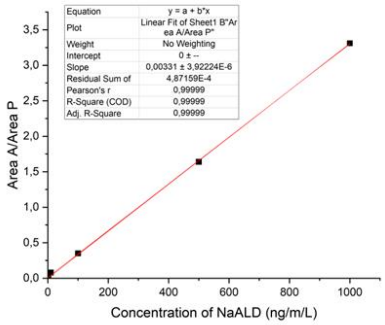

Figure 28: Calibration curve for NaALD in urine.

4.1.1. Selectivity

The selectivity of the method was illustrated by comparing chromatograms from the analysis of calibration samples with chromatograms of blank urine. No peaks with retention times close to those of the target analyte and internal standard were detected.

Figure 29 shows a chromatogram of a urine sample that does not contain the investigated substances. Figure 30 presents a chromatogram of a calibration sample with a concentration of alendronate 400 ng/mL and pamidronate 10 ng/mL, while Figure 31 shows a chromatogram of a urine sample from a rat treated with SDEDDS-NaALD.

4.1.2. Sensitivity

The lower limit of quantification (LLOQ) was established at 1 ng/mL with a coefficient of variation (CV) of ~17.4%, while the limit of detection (LOD) was 0.5 ng/mL.

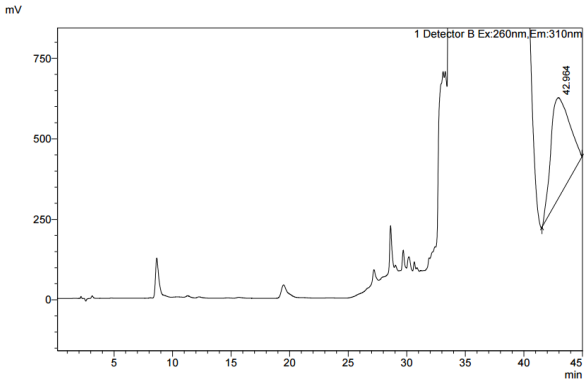

Figure 29: Chromatogram of alendronate-free urine sample (blank)..

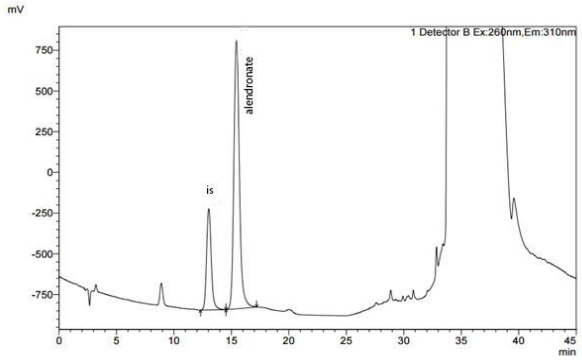

Figure 30: Chromatogram of urine sample spiked with standard solutions of NaALD and pamidronate (internal standard - IS) at 500 ng/mL..

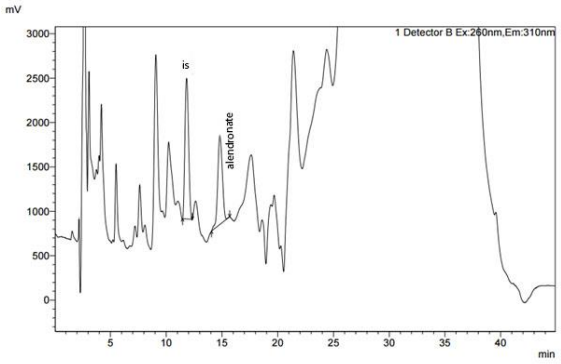

Figure 31: Chromatogram of urine sample from a rat treated with SDEDDS-NaALD, spiked with pamidronate as internal standard.

4.1.3. Accuracy and Precision

- Intra-day Accuracy and Precision

For each concentration level, five samples were analyzed. The results are presented in Table 24. The method precision, expressed as CV%, was below 8.4% across the entire concentration range for intra-day measurements.

Table 24: Intra-day accuracy and precision

	St 40 ng/L	St 100 ng/L	St 400 ng/L
	40,43	91,14	403,39
	39,01	91,65	344,04
	38,71	90,97	368,19
	40,52	109,62	371,59
	40,18	97,35	389,81
N	**5**	**5**	**5**
Medium	39,77	96,15	375,40
SD	0,85	7,99	22,59
Ac%	99,43	96,15	93,85
CV%	2,13	8,31	6,02
C_{nom}	**40,0**	**100**	**400**

- Inter-day Accuracy and Precision

Over three consecutive days, five samples from three concentration levels were analyzed each day. The results are presented in Table 25.

Table 25: Inter-day accuracy and precision from preliminary testing

	St 40,0 ng/L	St 100 ng/L	St 400 ng/L
	42,48	103,46	394,17
I day	44,17	99,42	374,43
	38,06	96,08	386,86
	40,23	101,03	393,78
	39,36	109,32	385,68
	41,87	85,75	356,98
II day	41,06	84,75	348,72
	38,94	85,77	434,79
	37,40	90,56	378,71
	38,88	106,00	360,17
	42,90	102,24	401,69
III day	42,54	90,62	390,43
	38,51	101,25	358,48
	42,14	104,30	391,93
	40,20	105,09	386,06
N	**15**	**15**	**15**
Medium	40,58	97,71	382,86
SD	2,04	8,19	21,56
Ac%	100,5	105,09	96,52
CV%	5,02	8,38	5,63
C_{nom}	**40,0**	**100**	**400**

The method's inter-day precision was below 8.4%, while accuracy exceeded 96% across the entire concentration range.

4.2. Assessing the oral bioavailability of NaALD from SDEDDS by quantifying drug excretion in urine of male Wistar rats

For drugs excreted predominantly unchanged in urine, bioavailability can be evaluated by measuring the total amount of drug excreted following a single dose[45]. Alendronate is excreted unchanged in urine, which constitutes its primary elimination pathway, with only negligible amounts detected in feces[46]. An absorption assessment was conducted by determining the excreted drug quantity in urine after oral administration of the different model formulations, with comparison to a reference standard[47]. The results of the HPLC analysis of urine samples are presented in Table 26.

In this pilot study, no significant difference was observed between the reference (FOS) and the SDEDDS model Smix1 3.0. The SDEDDS model PLG 1.1 demonstrated a 1.8-fold increase in absorption compared to the reference.

It can be concluded that the model formulation containing phosphatidylcholine enhances the permeability of NaALD. This result confirms the hypotheses derived from the in vitro studies using the PermeaPad® membrane. Further in-depth studies could validate the hypothesis that the PLG 1.1 model has the potential to increase the oral bioavailability of NaALD by promoting intestinal absorption.

[45] Le, J. (2022) 'Overview of pharmacokinetics', Skaggs School of Pharmacy and Pharmaceutical Sciences, University of California: San Diego, CA, USA

[46] Watts, N.B. and Diab, D.L. (2010) 'Long-Term use of bisphosphonates in osteoporosis,' The Journal of Clinical Endocrinology & Metabolism, 95(4), pp. 1555–1565. https://doi.org/10.1210/jc.2009-1947

[47] Han, H.-K., Shin, H.-J. and Ha, D.H. (2012) 'Improved oral bioavailability of alendronate via the mucoadhesive liposomal delivery system', European Journal of Pharmaceutical Sciences, 46(5), pp. 500–507. https://doi.org/10.1016/j.ejps.2012.04.002

Table 26. Alendronate concentrations (ng/mL) obtained from urine analysis of male Wistar rats.

No.	name	Delivered quantity (mg)	Urine volume (mL)	Peaks ratio	Concentration in the urine (ng/mL)	Total quantity found (ng)
1	CG (+) 1	1,5 (2,5 mg/mL)	4,9	0,039	11,77	57,66
2	CG (+) 2	1,5 (2,5 mg/mL)	12	0,125	37,83	453,96
3	CG (+) 3	1,5 (2,5 mg/mL)	3,2	0,025	7,68	24,59
4	PLG 1.1 (-) 1	0	12	-	under LOQ	-
5	PLG 1.1(+) 1	1,25 (2,5 mg/mL)	6	0,025	7,61	45,69
6	PLG 1.1 (-) 2	0	1	-	under LOQ	-
7	PLG 1.1 (+) 2	1,0 (2,5 mg/mL)	13	0,099	29,98	389,70
8	PLG 1.1 (-) 3	0,0	28	-	under LOQ	-
9	PLG 1.1 (+) 3	1,25 (2,5 mg/mL)	2,4	0,074	22,40	53,77
10	Smix1 3.0 (–) 1	0,0	5,8	-	under LOQ	-
11	Smix1 3.0 (+) 1	1,0 (2,5 mg/mL)	3,1	0,059	17,94	55,61
12	Smix1 3.0 (-) 2	0,0	40	-	under LOQ	-
13	Smix1 3.0 (+) 2	1,25 (2,5 mg/mL)	6,2	0,007	2,08	12,87
14	Smix1 3.0 (-) 3	0,0	28	-	under LOQ	-
15	Smix1 3.0 (+) 3	1,25 (2,5 mg/mL)	12,5	0,058	17,54	219,25

Table 27 presents the summarized results of the study.

Table 27: Amount of NaALD excreted in urine over a 48-hour period (mean value ±SD, n=3)

	Total amount found in the urine, ng	% of administered dose excreted in urine
Aqueous dispersion, reference (CG)	178,73±1,33	0,012±0,007
Model PLG 1.1	163,053±1,33	0,025±0,008
Model Smix1 3.0	95,91±1,33	0,011±0,008

V. CONCLUSIONS

1. SDEDDS models suitable for oral delivery of NaALD were developed, based on coconut oil, polysorbate 80, sorbitan monooleate, phosphatidylcholine, gelatin, and water. The optimal NaALD loading in SDEDDS was determined to be 7% (w/w).
2. The optimized SDEDDS models containing NaALD self-emulsify into w/o/w microemulsions, demonstrating bimodal size distribution of the dispersed phase in aqueous medium (0.1N HCl).
3. The developed formulations are compatible with NaALD, showing both physical and thermodynamic stability. At room temperature (20°C) they exhibit non-Newtonian fluid behavior, while at elevated temperatures (70°C) they behave as Newtonian fluids.
4. When formulated into hard gelatin capsules, the SDEDDS-NaALD concentrates meet pharmacopeial requirements for uniformity of mass of single-dose preparations (2.9.5) and uniformity of dosage units for single-dose preparations (2.9.40).
5. The self-emulsification time of SDEDDS-NaALD in hard gelatin capsules corresponds to the average gastric transit time of dosage forms under fasting conditions. Under these conditions, the concentrates self-emulsify in pH 1.6 medium to form microemulsions with bimodal droplet size distribution, while in pH 6.5 medium they form nanoemulsions with multimodal droplet size distribution.
6. The hard gelatin capsule models containing SDEDDS-NaALD release the active pharmaceutical ingredient according to the Korsmeyer-Peppas kinetic model when tested in a diffusion model with biomimetic membrane.
7. The oral bioavailability of NaALD from hard gelatin capsules containing SDEDDS, as determined by monitoring the excreted drug amount in urine of male Wistar rats, shows a 1.8-fold increase compared to the reference for the model based on polysorbate 80, coconut oil, phosphatidylcholine, sorbitan monooleate and gelatin (PLG1.1).

VI. CONTRIBUTIONS

Theoretical Scientific Contributions

1. For the first time, chemically, physically, and thermodynamically stable SDEDDS with NaALD (7% w/w) have been formulated, based on coconut oil, polysorbate 80, sorbitan monooleate, phosphatidylcholine, gelatin, and water, which self-emulsify in aqueous medium (0.1N HCl) into microemulsions.

Applied Scientific Contributions

1. The application of a UV-Vis spectrophotometric method for quantitative determination of NaALD incorporated in lipid-based drug delivery systems has been validated through complex formation with Fe^{3+}.
2. The diffusion model with a biomimetic membrane for investigating NaALD permeation from SDEDDS is suitable for predicting the system's in vivo behavior.
3. For the first time, an approach has been developed for incorporating NaALD into SDEDDS with enhanced drug permeability across biological membranes.
4. The developed approach for incorporating NaALD into SDEDDS with improved drug permeability across biological membranes is suitable for scaling under industrial conditions.

VII. PUBLICATIONS RELATED TO THE DISSERTATION RESEARCH

Publications in scopus-indexed journals

1. Pehlivanov I. Self-emulsifying drug delivery systems (SEDDS): excipient selection, formulation and characterization. Journal of IMAB. 2020 Jul-Aug;26(3). https://doi.org/10.5272/jimab.2020263.3226 (SJR 0.115)
2. Pehlivanov I., Nikolova Kr., Andonova V. Evaluation of the influence of some polymers on the physical stability of lipid self-double-emulsifying systems with Alendronate Sodium. Proceedings of Science. 2023 Oct 02. (SJR 0.115)

Publications in refereed national journals

3. Pehlivanov I., Sotirova Y., Dangova M., Andonova V. Self-Emulsifying Drug Delivery Systems as an Approach to Improved Oral Bioavailability of Drugs. Varna Medical Forum. 2022;11(2). doi:10.14748/vmf.v11i0.8981 (Indexed in national reference list).

VIII. PARTICIPATION IN SCIENTIFIC FORUMS RELATED TO THE DISSERTATION RESEARCH

1. I. Pehlivanov, Kr. Nikolova, V. Andonova. Evaluation of the influence of gelatin and lecithin on the physical stability of lipid self-double-emulsifying systems containing sodium alendronate. 8th Congress of Pharmacy with International Participation, April 27-30, 2023, "Rila" Hotel, Borovets Resort, Bulgaria. (Poster presentation)

2. I. Pehlivanov, Kr. Nikolova, V. Andonova. Evaluation of the influence of some polymers on the physical stability of lipid self-double-emulsifying systems with Alendronate Sodium. 11th International Conference of the Balkan Physical Union, August 28 - September 1, 2022, Belgrade, Serbia. (Oral presentation, Abstract S13-BMP-109)
3. I. Pehlivanov, Y. Sotirova, M. Dangova, V. Andonova. Self-emulsifying drug delivery systems as an approach to improve oral drug bioavailability. 10th Scientific Session with International Participation "80 Years of Medical College - Varna", September 20-21, 2022, Varna, Bulgaria. (Oral presentation)

IX. NOTED CITATIONS (EXCLUDING SELF-CITATIONS)

Article:

Pehlivanov I. Self-emulsifying drug delivery systems (SEDDS): excipient selection, formulation and characterization. Journal of IMAB. 2020 Jul-Aug;26(3). https://doi.org/10.5272/jimab.2020263.3226

Citation:

1. Poudwal, S. and Shende, P., 2022. Multi-strategic approaches for enhancing active transportation using self-emulsifying drug delivery system. Journal of Drug Targeting, 30(7), pp.726-736.
2. Gołdyn, M., Komasa, A., Pawlaczyk, M., Lewandowska, A. and Bartoszak-Adamska, E., 2021. Salts of purine alkaloids caffeine and theobromine with 2,6-dihydroxybenzoic acid as coformer: structural, theoretical, thermal and spectroscopic studies. Crystal Structure Communications, 77(11), pp.713-724.
3. Bodnar, L., Polovko, N., Bevz, N., Hrudko, V. and Perepelytsia, O., 2023. Biopharmaceutical justification of the creation of self-emulsifying drug delivery systems with simvastatin. ScienceRise: Pharmaceutical Science, (2(42)), pp.4-10.
4. Darusman, F., Dwiatama, A. and Priani, S.E., 2023. Formulasi dan Karakterisasi SelfNanoemulsifying Drug Delivery System (SNEDDS) Esomeprazol Magnesium Trihidrat.
5. Madhuri, D., 2023. Design and Development of Self-Emulsifying Drug Delivery Systems of Tolvaptan. Asian Journal of Pharmaceutics (AJP), 17(2).
6. Aishwarya, N. and ul Haq, S.M.F., 2022. Formulation and Evaluation of Solid-Self Nano Emulsifying Drug Delivery System of Darunavir. Saudi J Med Pharm Sci, 8(10), pp.558-574.

X. PARTICIPATION IN RESEARCH PROJECTS AND FUNDING

Part of the research was funded by the "NAUKA" fund project № 22023:
"Evaluation of Pharmacokinetic Parameters of Self-Double-Emulsifying Drug Delivery Systems with Sodium Alendronate for Oral Administration"
Project Leader: Assoc. Prof. Velichka Yordanova Andonova, PhD

XI. ACKNOWLEDGEMENTS

First and foremost, I would like to express my deepest gratitude to my scientific supervisors - Assoc. Prof. Velichka Andonova and Prof. Kaloyan Georgiev!

I thank Assoc. Prof. Velichka Andonova for her patience, sleepless nights, unwavering support, and invaluable guidance throughout the preparation of this dissertation!

I thank Prof. Kaloyan Georgiev for his assistance and advice in planning and preparing the pharmacokinetic animal experiments!

I am grateful to the Department of Pharmacology, Toxicology, and Pharmacotherapy for providing me the opportunity to develop this dissertation under their auspices!

I extend my thanks to the Department of Pharmaceutical Technologies for granting me access to their laboratory facilities to conduct the experimental work for my thesis!

I offer heartfelt gratitude to Prof. Kostena Nikolova for her help with statistical analysis, physical and thermodynamic modeling, and interpretation of some results.

Special thanks to Assistant Prof. Stefan Stefanov and Senior Assistant Prof. Stella Dragomanova, who stood by me during those hot summer days spent in the vivarium! I also thank Dr. Krasimir Kuzmanov for his valuable practical advice!

I am indebted to Senior Assistant Prof. Kristina Bozhinova for her assistance with chromatographic analyses.

I thank Assoc. Prof. Stefka Titeva, Prof. Nikolay Lambov, Prof. Milen Dimitrov, and Prof. Krum Kafedzhiyski for their encouragement and guidance during our meetings and discussions throughout this endeavor!

I acknowledge all colleagues and friends who, in one way or another, contributed to the completion of this dissertation!

Lastly, I express my immense gratitude to my family for their unwavering support and patience during my entire doctoral journey!